



VERIFICATION AND OPTIMIZATION OF NONLINEAR SHELL BUCKLING
FORMULA OF THIN-SHELL STRUCTURES

Jie Xu

Student Number: 4701732

VERIFICATION AND OPTIMIZATION OF NONLINEAR SHELL BUCKLING
FORMULA OF THIN-SHELL STRUCTURES

by

Jie Xu
Student Number: 4701372

ADDITIONAL GRADUATION WORK

Submitted in partial fulfillment of the requirements for the degree of

MASTER OF SCIENCE

in

Delft University of Technology

Supervisors:

Dr. ir. P. C. J. Hoogenboom
Dr. ir. C. van der Veen



Preface

By taking shell buckling as the research subject I could be able to gain a better comprehension of shell buckling behavior, at the same time, I could also gain 10 ECTs to take the report as the assignment of CIE5050-09 (*Additional Graduation Work, Research Project*) in Delft University of Technology.

This report is intended for engineers that are facing to designs of shell structures and students to help them gain a better understanding of shell buckling behavior.

Appreciation to Dr. Hoogenboom and Dr. van der Veen for their patience and generous help.
Appreciation to Zhenheng Kong and Jijia Que for lending me their lap-tops.

VERIFICATION AND OPTIMIZATION OF NONLINEAR SHELL BUCKLING FORMULA OF THIN-SHELL STRUCTURES

Author: Jie Xu

Student Number: 4701372

E-mail Address: J.Xu-10@student.tudelft.nl

SUMMARY

Shell is a popular form of structures as it can withstand relative large load with small thickness, which satisfies the aesthetic preference. Due to the curvatures of shell structures, shell can carry the distributed load as membrane forces instead of bending moments. Due to the small thickness, shell structures are highly sensitive to imperfections. As the loads are carried by membrane forces, buckling failure often govern the design of shell structures. The buckling load could be predicted accurately by performing a nonlinear finite element analysis. However, performing a nonlinear finite element analysis is very time-consuming and expensive as a lot of computational efforts required. The currently used design formula of shell structures can lower down the requirement of computation in a great degree while the accuracy is not very satisfying.

Different from other types of structures, shell buckling often starts locally, therefore, an assumption is made that shell buckling is a combination of membrane forces and curvatures. Thus, an improved buckling formula is proposed. In this report, the proposed formula is verified and optimized. In addition, the shell behavior before buckling has been illustrated by a series of figures that show the deformation and stresses at several load steps.

Supervisors:

Dr. ir. P. C. J. Hoogenboom

Dr. ir. C. van der Veen

Contents

1 INTRODUCTION	5
1.1 Thesis Statement	5
1.2 Research Purpose	5
1.3 Research Method	5
1.4 Literature	5
1.5 Thesis Overview	6
2 BACKGROUND	7
2.1 Shell Linear Elastic Theory	7
2.1.1 Coordinate Systems and Curvatures	7
2.2 Shell Buckling	10
2.2.1 Static Instability	10
2.2.2 Bifurcation Buckling	11
2.2.3 Imperfection Sensitivity	11
2.3 FEM	13
2.3.1 Finite Element Implementation	13
2.3.2 FEM Solution Techniques	14
2.4 Initial Imperfections	15
2.5 Proposed Formula	16
3 METHODS	17
3.1 Model Creation	17
3.1.1 Shape of Shell Structures	17
3.1.2 Nodes	19
3.1.3 Elements	19
3.1.4 Boundary Conditions	21
3.2 Mechanical Analysis	22
3.2.1 Linear Buckling Analysis (LBA)	22
3.2.2 Geometrically Nonlinear Analysis with Initial Geometric Imperfections (GNIA)	22
4 RESULTS	28
4.1 GNIA Results	28
4.2 Curvatures	29
4.3 Thickness	30
4.4 Young's Modulus	31
4.5 Buckling Procedures	31
4.5.1 Displacements	31
4.5.2 The Third Principal Stresses	32
5 DISCUSSION AND CONCLUSION	36
5.1 Discussion of the Correctness of the Results	36
5.2 Discussion of the Scatter Diagrams	36
5.2.1 Curvatures	36
5.2.2 Thickness	36
5.2.3 Young's Modulus	36

5.2.4	Conclusion	37
5.3	Recommendations for Further Research	37
A	Command Lines of ANSYS Mechanical APDL (modified from [17])	40
B	Curvatures	46
C	Thickness	59
D	Young's Modulus	60

List of Figures

1	Coordinate systems[10]	7
2	Normal section curvature[10]	8
3	Positive internal forces	9
4	Load-deflection curves showing limit and bifurcation points: (a) General nonlinear analysis, and (b) Asymptotic analysis[7, 17]	10
5	Test results of axially loaded cylinders[20, 17]	11
6	(a) Postbuckling and imperfection sensitivity of externally pressurized cylinder, and (b) Imperfection sensitivity of various shells (modified from [6])[17]	12
7	Flat shell element[10]	14
8	Semi-loof element[10]	14
9	Reduced solid element[10]	14
10	Cylinder	17
11	Thin-shell cylinder imperfection sensitivity[17]	18
12	Element type and material properties	18
13	Code of node creation	20
14	Element creation	21
15	Element creation code	22
16	Shell281 Geometry[2]	23
17	Code of boundary conditions	23
18	Model	24
19	Linear elastic analysis (LE) code	24
20	Linear buckling analysis (LBA) code	24
21	First linear buckling modes of the example cylinder	25
22	Get maximum deflection code	25
23	Transformation Matrix	26
24	Update the geometry code	26
25	Geometrically nonlinear analysis code	27
26	Contour plot of the displacements of the example cylinder	28
27	Contour plot of the third principal stresses of the example cylinder	28
28	Membrane forces-displacement diagram of the example cylinder under GNIA	29
29	Nonlinear buckling membrane forces-sum of curvatures scatter diagram	29
30	Nonlinear buckling membrane forces-radius scatter diagram	30
31	Nonlinear buckling membrane forces-thickness scatter diagram	30
32	Nonlinear buckling membrane forces-Young's modulus diagram	31
33	Undeformed cylinder with initial geometric imperfections	32
34	Deformation development of the example cylinder	32
35	Deformation of the example cylinder when buckling occurs	33
36	The third principal stresses of the example cylinder (Phase 1)	33
37	The third principal stresses of the example cylinder (Phase 2)	34
38	The third principal stresses of the example cylinder (Phase 3)	34
39	The third principal stresses of the example cylinder (Phase 4)	35
40	The third principal stresses of the example of cylinder (Phase 5)	35

List of Tables

1	Shell types and corresponding theory based on radius a and thickness t[10, 17]	9
2	Nonlinear buckling membrane forces-sum of curvatures	46
3	Nonlinear buckling membran forces-thickness	59
4	Nonlinear buckling membrane forces-Young's modulus	60

1 INTRODUCTION

1.1 Thesis Statement

Shells tend to be thin because their curvature enables them to carry distributed load as membrane forces[17]. Therefore, shell is a quite popular form of structures as it can withstand relative large load with small thickness, which satisfies the aesthetic preference. By taking load as membrane forces, buckling failure often govern the design of shell structures. At the same time, due to the small thickness, shell structures are extremely sensitive to imperfections.

With nonlinear finite element analysis (NLFEA), the buckling load could be predicted accurately. However, nonlinear finite element analysis is extremely time-consuming as there are a lot of computational efforts are required, also very expensive. The currently used design formula could help gain results easily, however, the accuracy is not very satisfying.

Different from other forms of structures, shell buckling often starts locally, therefore, an assumption is made that shell buckling is a combination of membrane forces and curvatures. Thus, a new design formula is proposed.

1.2 Research Purpose

The research purpose of this report is to verify and optimize the following formula for shell buckling.

$$n_{xx} + n_{yy} = -0.1Et^2 \frac{k_{xx} + k_{yy}}{2} \quad (1)$$

where E is the Young's modulus, t is the shell thickness, k_{xx} and k_{yy} are the curvatures of shell structures in x and y direction and n_{xx} and n_{yy} are the membrane forces in the x and y direction.

An additional research purpose is to understand and explain the shell behavior before buckling.

1.3 Research Method

The program ANSYS Mechanical APDL has been used to generate cylinder shells of different size. The shells were analyzed by a geometrical nonlinear procedure that increases an axial edge load in small steps until buckling occurs. A database has been made of the buckling membrane forces. The database was imported into MatLab and the proposed formula was verified and optimized.

1.4 Literature

The new design formula (Eq.1) is proposed by Dr. ir. P. C. J. Hoogenboom in meeting with the author.

The APDL script used in this report is based on the APDL script used in the report of E. J. Giesen Loo[17]. Loo also quantifies the influence of the initial geometric imperfections to the toroidal shell segments. He also found that for toroidal shell segments, edge disturbance occurs at the locations where Gaussian curvature equals to zero[17].

1.5 Thesis Overview

In this report, there are 5 chapters in total.

Chapter 2 introduces the basic theories that used in this report.

In Chapter 3, the methods used in this report are elaborated. Command batches are illustrated and elaborated separately.

In Chapter 4, the results and the figures that illustrate shell behavior before buckling are listed.

In Chapter 5, the results are discussed and a conclusion of the formula is drawn.

2 BACKGROUND

2.1 Shell Linear Elastic Theory

2.1.1 Coordinate Systems and Curvatures

Shells can be described as plates with a curved middle surface. This curvature enables shells to carry out-of-plane pressure loads as membrane forces instead of bending moments[3, 19, 17]. The latter are restricted to so-called edge disturbances found at concentrated loads, edges and any other discontinuities[19, 10, 17].

In order to describe the shell structures mathematically, the coordinate systems are used, thus, the curvatures could be derived and Lamé parameters are introduced. In shell analysis three coordinate systems are used: 1) a global coordinate system to describe the shape of the shell, 2) a local coordinate system to define curvature, displacements, membrane forces, moments and loading, 3) a curvilinear coordinate system to derive and solve the shell equations[10].

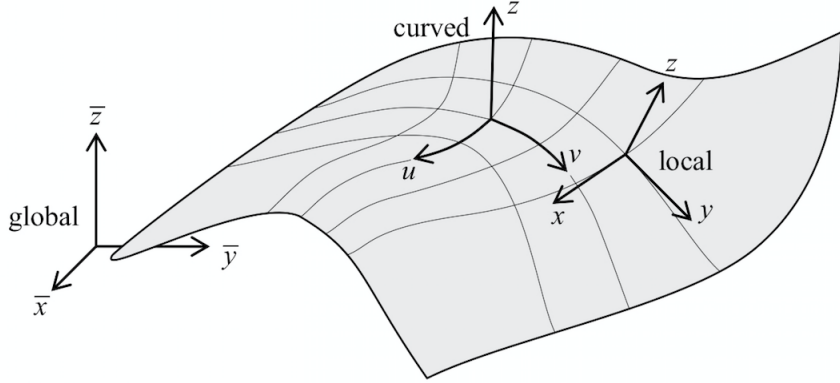


Figure 1: Coordinate systems[10]

Curvature is also defined for surfaces. The \$z\$ axis is a part of a local coordinate system. When the normal plane includes the \$x\$ direction vector the curvature is \$k_{xx}\$. When the plane includes the \$y\$ direction vector the curvature is \$k_{yy}\$. These curvatures can be calculated by[10]

$$k_{xx} = \frac{\partial^2 z}{\partial x^2} \quad (2)$$

$$k_{yy} = \frac{\partial^2 z}{\partial y^2} \quad (3)$$

and

$$k_{xy} = \frac{\partial^2 z}{\partial x \partial y} \quad (4)$$

There are many possible normal planes of a point of a surface, and therefore, the principal curvatures at this point could be calculated as Eq.5[10].

$$k_{1,2} = \frac{1}{2}(k_{xx} + k_{yy}) \pm \sqrt{\frac{1}{4}(k_{xx} - k_{yy})^2 + k_{xy}^2} \quad (5)$$

The mean curvature of a surface at a point is half the sum of the principal curvatures at this point $k_m = \frac{1}{2}(k_1 + k_2)$. It can be shown that also $k_m = \frac{1}{2}(k_{xx} + k_{yy})$. The mean curvature is independent of how we choose the local coordinate system except for the direction of z axis[10].

$$\alpha_x = \frac{dx}{du} \quad (6)$$

$$\alpha_y = \frac{dy}{dv} \quad (7)$$

The Lamé parameters α_x and α_y maps the ratio of the change in x with respect to the change in u and a change in y with respect to a change in v [10, 17].

The in-plane curvatures k_x and k_y are defined as Eq.8 and Eq.9.

$$k_x = \frac{1}{\alpha_x} \frac{\partial \alpha_x}{\partial y} \quad (8)$$

$$k_y = \frac{1}{\alpha_y} \frac{\partial \alpha_y}{\partial x} \quad (9)$$

If the shell is parameterized, the Lamé parameters can be used to derive k_{xx} , k_{yy} and k_{xy} [17].

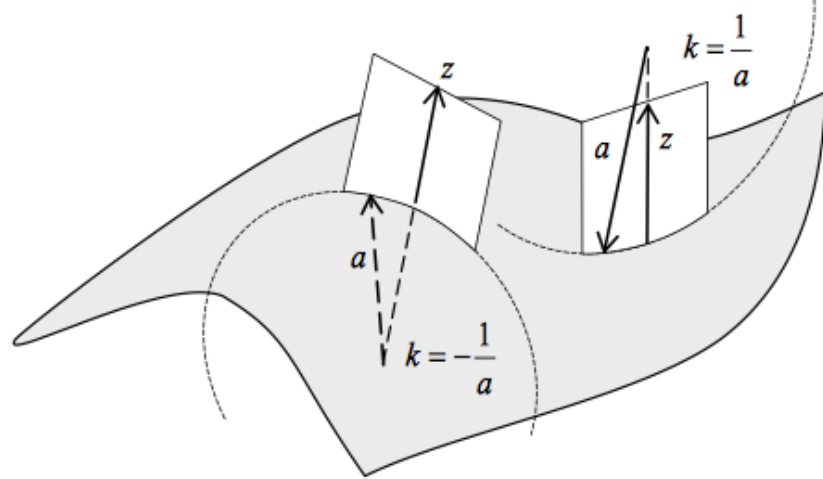


Figure 2: Normal section curvature[10]

Table 1: Shell types and corresponding theory based on radius a and thickness t [10, 17]

Type of Shell	Slenderness	Theory
Very thick shell	$a/t < 5$	Solid elements (i.e., not a shell)
Thick shell	$5 < a/t < 30$	Mindlin-Reissner (includes shear deformation)
Thin shell	$30 < a/t < 4000$	Sanders-Koiter (membrane forces and moments)
Membrane	$4000 < a/t$	Shell membrane (only membrane forces)

The geometry of a shell is described by its thickness and surface curvature. Thus, shell can be categorized based on their radius-to-thickness ratio[3, 17]. Table 1 shows such a classification, with suitable theories[17].

As seen in Table 1, the analysis of thin shells involves two distinct theories: the shell membrane theory, which does not include bending and shear, and the Sanders-Koiter theory, which includes bending deformation and shear stresses but not shear deformation[19, 17]. The positive internal force resultants from the latter theory are shown in Fig.3[17].

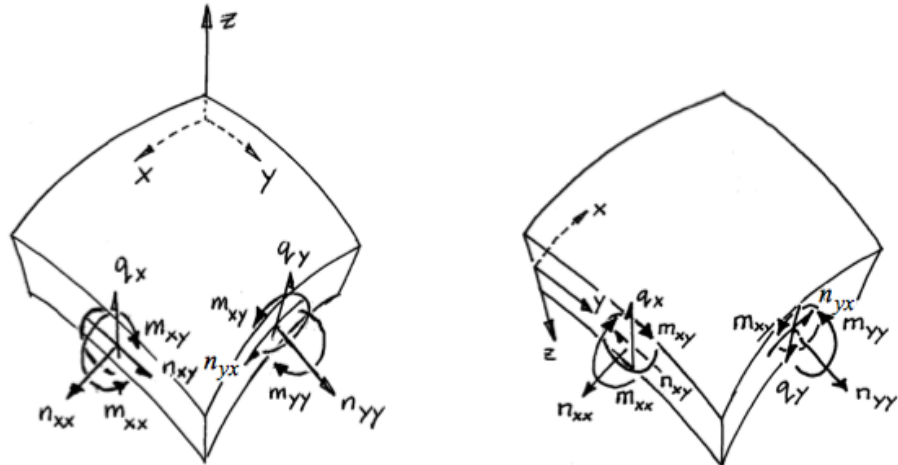


Figure 3: Positive internal forces

Even though the Sanders-Koiter equations offer a more faithful representation of internal forces of shell structures, membrane stresses are more important for practical purpose[19, 17]. The shell membrane equations are also simpler to solve analytically. This solution required only the shell membrane equilibrium euqation shown next[10, 3, 17].

$$\frac{\partial n_{xx}}{\partial x} + \frac{\partial n_{xy}}{\partial y} + k_y(n_{xx} - n_{yy}) + 2k_x n_{xy} + p_x = 0 \quad (10)$$

$$\frac{\partial n_{yy}}{\partial y} + \frac{\partial n_{xy}}{\partial x} + k_x(n_{yy} - n_{xx}) + 2k_y n_{xy} + p_y = 0 \quad (11)$$

and

$$k_{xx}n_{xx} + 2k_{xy}n_{xy} + k_{yy}n_{yy} + p_z = 0 \quad (12)$$

2.2 Shell Buckling

Shells tend to be thin because their curvature enables them to carry distributed load as membrane forces. The property of thinness stems from shells' capacity to store membrane strain energy without much deformation. Yet, if this energy is converted into bending energy, shells may become statically unstable and fail dramatically[7, 17].

2.2.1 Static Instability

Static instability, loosely termed buckling, is the condition when a structural member or system exhibits a loss in its load-carrying capacity[21, 17]. Buckling may be divided into two categories: 1) bifurcation of equilibrium (Fig.4, point B) and 2) collapse at the limit load without prior bifurcation (point A). Bifurcation is exemplified by a sudden change in the load-carrying path, e.g., from axial (or membrane) forces to bending moment, and corresponding deformations. Columns, plates and cylindrical shells experience this type of instability. Shallow arches and spherical caps are example of the second type of instability, also termed nonlinear buckling or "snap-through"[21, 7, 17]. However, given initial geometric imperfections, even arches and spherical caps are prone to fail in an asymmetric mode due to bifurcation prior to their limit load, i.e., curve 0-B-D in Fig.4[21, 13, 7, 17].

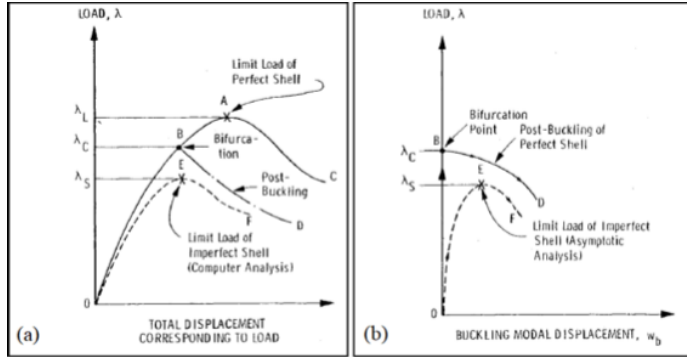


Figure 4: Load-deflection curves showing limit and bifurcation points: (a) General nonlinear analysis, and (b) Asymptotic analysis[7, 17]

The loads observed in Fig.4 are expressed as a multiplier λ to some reference load. λ_C is the critical buckling load ratio at the bifurcation point. λ_L , or limit load ratio, is the maximum load that can be achieved without prior bifurcation. λ_S is the maximum load that can be achieved by a structure with initial geometric imperfections before static instability is reached[13, 17]. Chapter 1 refers to λ_S as the nonlinear buckling load because – just like for the limit load ratio – λ_S is obtained by means of a geometrically nonlinear analysis (GNA). However, estimating λ_S requires explicit modeling of the initial geometric imperfections in the finite element model. An analysis

that includes such imperfections is referred to as a geometrically nonlinear analysis with initial geometric imperfections (GNIA)[17].

2.2.2 Bifurcation Buckling

The critical buckling load for discretized systems is the lowest eigenvalue from

$$n_C = -[3(1 - \nu^2)]^{-1/2} \frac{Et^2}{a} \cong -0.6 \frac{Et^2}{a} \quad (13)$$

$[3(1 - \nu^2)]^{-1/2}$ is approximated as 0.6 for realistic value of ν . Eq.13 is also valid for axially loaded hyperboloids and for externally pressurized closed cylinders, spherical shells, domes, and hyperbolic paraboloids[10, 17]. The fact that Eq.13 makes no reference to the number of waves found in the buckling pattern helps to explain this wide range of applicability[7, 17]. This quality has further repercussions seen in subsection 2.2.3 which describes methods that estimate λ_S based on asymptotic analyses that rest on the theoretical foundations established by Koiter and use the postbuckling behavior as a starting point[13, 17].

2.2.3 Imperfection Sensitivity

The classical example of imperfection sensitivity is the axially loaded thin-shell cylinder[10, 20, 17]. Fig.5 shows the test results of 172 axially loaded thin-shell cylinders compared to the critical load predicted by Eq.13. n_S has values as low as one sixth of n_C . Kármán and Tsien attributed this discrepancies to the highly unstable postbuckling regimes seen in both cylindrical and spherical shells[15, 17].

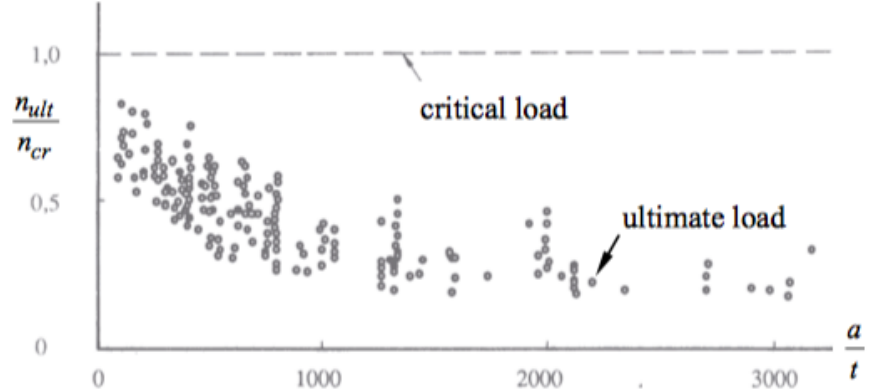


Figure 5: Test results of axially loaded cylinders[20, 17]

Around the same time, Koiter found that asymptotically exact estimates λ_S can be obtained by including the first-order effects of small initial geometric imperfections in the shape of the critical buckling mode[13, 7]. If the magnitude of the initial geometric imperfection is denoted as $\bar{\delta}$, then for $a_s = 0$ and $b_s < 0$, λ_S can be estimated by[17]

$$\lambda_S \cong \lambda_C [1 - 3(\frac{-b_s}{4})^{1/3} (\rho\bar{\delta})^{2/3}] \quad (14)$$

where ρ is a constant that depends on the imperfection shape. On the other hand, for a postbuckling curve with $a_s \neq 0$ and $b_s = 0$, λ_S is estimated using[17]

$$\lambda_S \cong \lambda_C [1 - 2(-\rho a_s \bar{\delta})^{1/2}] \quad (15)$$

In both cases, small values of $\bar{\delta}$ have a sizeable on λ_S [13, 17] which further substantiates the claim by Kármán and Tsien[15, 17].

2.2.3.1 Externally Pressurized Thin-Shell Cylinder

The externally pressurized thin-shell cylinder studied by Budiansky and Amazigo[5, 17] is an illustrative example of Koiter's theory. The solid curve on Fig.6 (a) represents the pressure-deflection relation of the perfect structure given by[17]

$$p = p_C [1 + b(\frac{\delta}{t})^2] \quad (16)$$

where p is the postbuckling pressure, p_C is the critical buckling pressure and δ is the normal to surface buckling displacement amplitude. In turn, the solid curve in Fig.6 (b) represent the asymptotic relationship between p_S and $\bar{\delta}$ given by Eq.17, which is the same form as Eq.14[17].

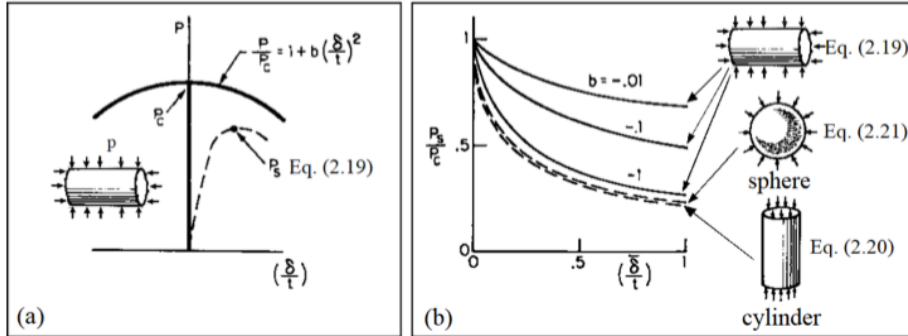


Figure 6: (a) Postbuckling and imperfection sensitivity of externally pressurized cylinder, and (b) Imperfection sensitivity of various shells (modified from [6])[17]

$$(1 - \frac{p_S}{p_C})^{3/2} = \frac{3\sqrt{3}}{2} (-b)^{1/2} \left| \frac{\bar{\delta}}{t} \right| \left(\frac{P_S}{P_C} \right) \quad (17)$$

However, Eq.13 and Eq.14 cannot be applied to the axially loaded thin-shell cylinder nor the externally pressurized spherical shell studied by Kármán and Tsien in 1941[14, 15, 17] due to the multiplicity of buckling modes associated with λ_C [6, 13, 7, 17]. The reader may recall that Eq.13 applicable to both cylinders and spheres – makes no mention of a buckling pattern, thus hinting at the fact these shells are susceptible to several mode-based geometric imperfections[7, 17].

2.2.3.2 Axially Loaded Thin-Shell Cylinder and Externally Pressurized Spherical Shell

Even with this limitation, it is possible to give a close estimate of P_S for the axially loaded thin-shell cylinder with the classical theory by using an imperfection in the shape of the axisymmetric buckling mode[16, 13, 17]:

$$(1 - \frac{P_S}{P_C})^2 = \frac{3c}{2} \left| \frac{\bar{\delta}}{t} \right| \left(\frac{P_S}{P_C} \right) \quad (18)$$

or

$$\frac{P_S}{P_C} = 1 + \frac{3c \bar{\delta}}{4 t} - \sqrt{\frac{3c \bar{\delta}}{4 t} (2 + \frac{3c \bar{\delta}}{4 t})} \quad (19)$$

where $c = \sqrt{3(1 - \nu^2)}$. Koiter also found that the cylinder's length and boundary conditions play a negligible role[16, 17]. Similarly, Hutchinson developed an equation for a shallow section of an externally pressurized spherical shell, taking in consideration the interaction between buckling modes[12, 17]. The highest reduction in pressure was observed for two operative buckling modes with one such mode having a zero wave-number associated with either the x or y coordinate[17]:

$$(1 - \frac{p_S}{p_C})^2 = \frac{27\sqrt{3}c}{32} \left| \frac{\bar{\delta}}{t} \right| \left(\frac{p_S}{p_C} \right) \quad (20)$$

or

$$\frac{p_S}{p_C} = 1 + \frac{27\sqrt{3}c \bar{\delta}}{64 t} - \sqrt{\frac{27c \bar{\delta}}{1024 t} (32\sqrt{3} + \frac{81c \bar{\delta}}{4 t})} \quad (21)$$

Equations 18, 19, 20 and 21 are plotted in Fig.6. Similar imperfection sensitivity studies were done on axially compressed oval thin-shell cylinder[12, 17], externally pressurized thin0shell spheroids[9, 17] and externally pressurized thin-shell toroidal segments[11, 17]. It appears that imperfection sensitivity disappears for toroidal segments of sufficiently large negative Gaussian curvature[6, 17].

2.3 FEM

2.3.1 Finite Element Implementation

The three most common shell finite elements are: flat shell elements, elements based on Sanders-Koiter equations and reduced solid elements[10, 17]. Flat shell elements combine plane stress with plate bending ad drilling degrees of freedom[10, 3, 17]. Their main disadvantage is that, by being flat, a fine mesh is required to preserve the curvature of the shell model[8, 17].

Shell elements based on the Sanders-Koiter equations, such as semi-loof element (Fig.8), can be very accurate but are often difficult to implement in finite element software[10, 17].

The most common element type is the reduced solid element (Fig.9) in which degrees of freedom are combined the constitutive equations are simplified[10, 3, 17]. 8-noded quadrilaterals can be curved, which reduces the need for fine meshes. The script provided in Appendix.A used this shell element to generate shell models.

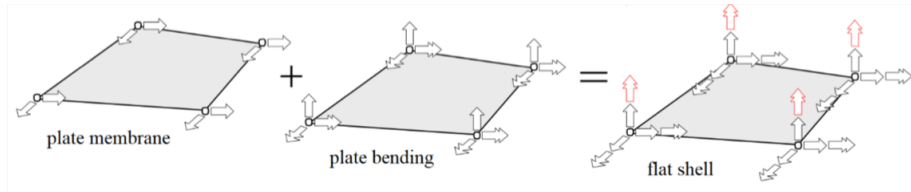


Figure 7: Flat shell element[10]

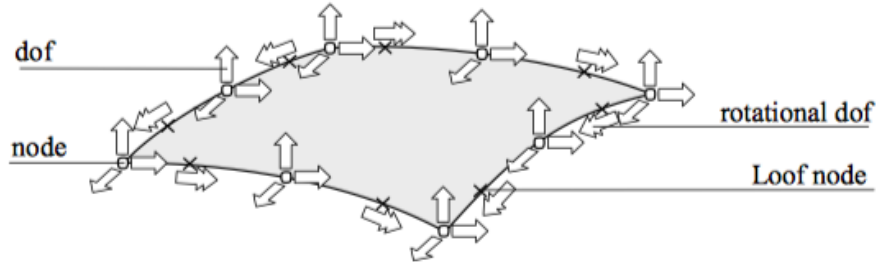


Figure 8: Semi-loof element[10]

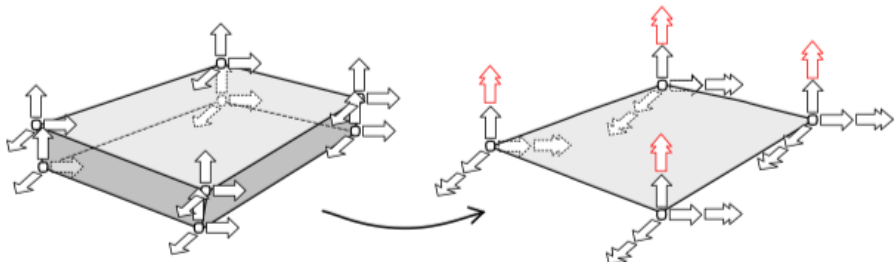


Figure 9: Reduced solid element[10]

2.3.2 FEM Solution Techniques

Two FEM procedures are described, each with its own strengths and pitfalls: linear buckling analysis (LBA) and geometrically nonlinear analysis (GNA). LBA is an eigenvalue analysis based on Eq.22[2, 18, 17]

$$(K + \lambda_i K_g) \Psi_i = 0 \quad (22)$$

where K is the (linear elastic) stiffness matrix, K_g is the geometric stiffness matrix computed for a reference load, λ_i is an eigenvalue (buckling load factor) and Ψ_i is a corresponding eigenvector (buckling mode). LBA assumes negligible deflections prior to bifurcation of the loading path[18, 17].

The lowest eigenvalue is referred to as the critical buckling load, that is, λ_C .

The assumption of negligible displacements seldom holds: the transition to an alternate load path is usually gradual due to deflections which may be enhanced or even triggered by the presence of initial geometric imperfections. GNA accounts for these deformation by updating the geometry and satisfying equilibrium on the deformed geometry[18, 17].

GNA commonly tracks the equilibrium path via an incremental-iterative scheme: equilibrium is established to prescribed tolerances by means of iterations at each load increment[18, 17]. The reader is referred to[4, 17] for a comprehensive treatment of such schemes. The script provided in App.A stipulates that analyses of this sort be executed using an arc-length controlled Newton-Raphson method.

While GNA can yield a good approximation of λ_L , it fails to capture the effect of initial geometric imperfections. GNA with explicitly modeled initial geometric imperfections is referred to as a GNIA. Such analyses are typically required for cases in which the initial geometric imperfections play a crucial role in triggering the nonlinear behavior and account for a significant reduction from λ_C to λ_S [17].

2.4 Initial Imperfections

Chen proposes four approaches to adding imperfections[8, 17]. The first approach is to update the geometry by rescaling the k^{th} buckling load. This is achieved via

$$\delta^{Imp}(u, v) = \frac{\bar{\delta}}{\delta_{max}^k} \delta^k(u, v) \quad (23)$$

where $\delta^{Imp}(u, v)$ is the imperfection, $\bar{\delta}$ is the prescribed magnitude, $\delta^k(u, v)$ is the deflection of the k^{th} buckling mode and δ_{max}^k is the absolute maximum of δ^k .

The second approach that suggested by Chen is to apply a uniform combination of n buckling modes based on[8, 17].

$$\delta^{Imp}(u, v) = \frac{\bar{\delta}}{max \sum_{k=1}^n \delta^k(u_i, v_j)} \sum_{k=1}^n \delta^k(u, v) \quad (24)$$

The denominator equals the maximum deflection of the sum of the n modes for all possible (u_i, v_j) .

Chen further suggests using[8, 17]

$$\delta^{Imp}(u, v) = \frac{\bar{\delta}}{\delta_{max}^{rand}} \delta^{rand}(u, v) \quad (25)$$

instead of Eq.24, because the contribution of each buckling mode is randomized.

The buckling modes are combined to yield δ^{rand} using[17].

$$\delta^{rand}(u, v) = \sum_{k=1}^n A^k \delta^k(u, v) \quad (26)$$

where

$$A^k = \text{rand}(0, 1), k \in [1, n] \quad (27)$$

The remaining two approaches suggested by Chen are using random noise imperfections, a drawback of which is its mesh dependency; and imperfection pattern based on sinusoidal waves[8, 17]. Only Eq.22 is implemented in the script in Appendix. However, using Eq.24 or Eq.25 could yield remarkable results as the first mode may not govern as shown by the axially-loaded thin-shell cylinder and externally pressurized spherical shell[6, 13, 17]. Chen also observed that for structures with closely spaces buckling loads the imperfection sensitivity tends to be significant and is often controlled by a combination of buckling modes[8, 17].

2.5 Proposed Formula

Different from other forms of structures, buckling of shells often start locally. Therefore, an assumption is made that the macro shape of shell structure only plays a negligible role in shell buckling. Shell buckling start at a location where a combination of curvature and membrane forces is met[17].

Therefore, a formula is proposed for the relationship between the critical membrane forces and curvatures for thin-shell structures.

$$n_{xx} + n_{yy} = -0.6Et^2 \frac{k_{xx} + k_{yy}}{2} \quad (28)$$

Due to shell structures are highly sensitive to imperfections, a factor that equals to $\frac{1}{6}$ is applied. Therefore, the proposed formula with consideration of imperfections is

$$n_{xx} + n_{yy} = -0.1Et^2 \frac{k_{xx} + k_{yy}}{2} \quad (29)$$

For the equations above, E is the Young's modulus of the material applied in the structures. t stands for the thickness of the shell.

3 METHODS

3.1 Model Creation

3.1.1 Shape of Shell Structures

In order to minimize the influence of the boundary conditions and edge disturbance due to the application of loads, axially-loaded cylinders are chosen for this report.

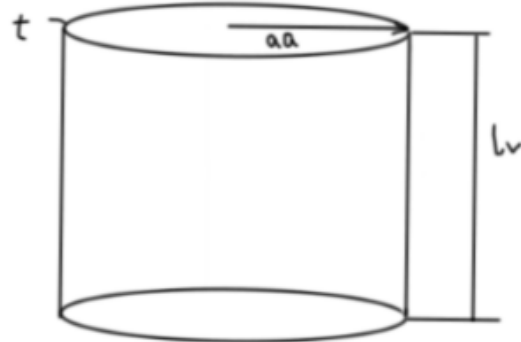


Figure 10: Cylinder

The translational displacements at the bottom edges of cylinders are restrained. Vertically uniform pressures are applied at both the top and bottom rings of cylinders to avoid the edge disturbance at the bottom edges.

In case of cylinders buckle in bending, the length of the cylinder l_v should equal to $10\sqrt{aa \cdot t}$ where aa is the radius of the cylinder, and t is the thickness of the cylinder.

At the same time, the radius-to-thickness ratio is limited between 30 and 1000 for this formula Eq.1

Due to the imperfection sensitivity of shell structures, the initial geometric imperfections should be taken into consideration. As shown in Fig.11, where δ is the predefined scale of the initial geometric imperfections, when the ratio $\frac{\delta}{t}$ increases, the λ decreases. And when the ratio $\frac{\delta}{t}$ goes infinite, the λ tends to be a constant. Therefore, in this report, $\delta = 5t$ is chosen as the predefined scale of the initial geometric imperfections.

As shown in Eq.1, the Poisson's ratio of the material does not occur in this equation, therefore, for all models used in this report, the Poisson's ratio is assumed to be 0.3.

The cylinder is parameterized by equations that model the inner walls of a cylinder; hence it is easy to change the mean curvatures of cylinders by changing the value of aa .

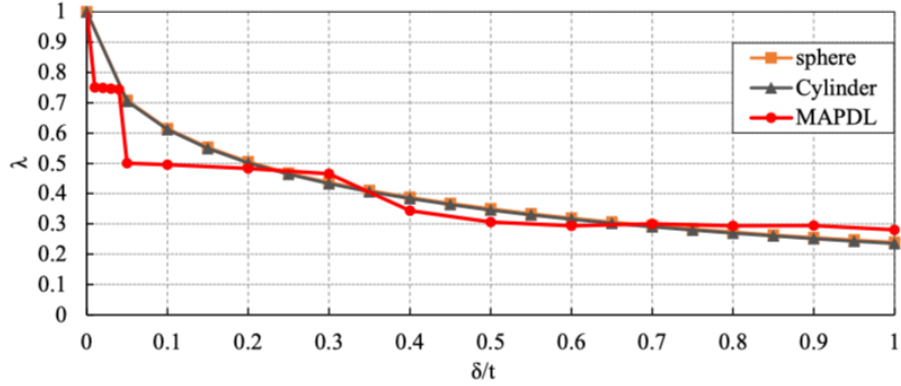


Figure 11: Thin-shell cylinder imperfection sensitivity[17]

The model uses reduced solid 8-noded quadrilateral shell elements (SHELL281) with thickness equals to t . The material is assumed to be linear-elastic with Young's modulus equals to E and Poisson's ratio equals to ν . The element type is defined with **ET**, the thickness is defined with **R** and the material properties are defined with **MP**. All commands (in bolds) are from ANSYS Inc[1, 17].

```

! Create element type: shell
!-----
ET, 1, SHELL281           ! element type: 8 node quadrilateral
R, 1, t, t, t, t,,        ! element thickness

! Create material properties
!-----
MP, EX, 1, E               ! Elastic modulus (linear elastic material)
MP, PRXY, 1, w              ! Poisson' s ratio (linear elastic material)

```

Figure 12: Element type and material properties

The script in Fig.12 defines the element type and material properties. Note that the Poisson's ratio is represented by w to avoid confusion between the v parameter and the Greek letter ν .

Cylinders could be parameterized by

$$r(u, v) = \begin{Bmatrix} \bar{x}(u, v) \\ \bar{y}(u, v) \\ \bar{z}(u, v) \end{Bmatrix} = \begin{Bmatrix} aa \cdot \cos(u) \\ aa \cdot \sin(u) \\ v \end{Bmatrix} \quad (30)$$

where v goes from 0 to $l_v = 10\sqrt{aa \cdot t}$ and u goes from 0 to 2π . The length l_v is the total height of the cylinder.

Subsections 3.1.2 and 3.1.3 illustrate the creation of nodes (**N**) and elements (**E**), respectively. Subsection 3.1.4 summarizes the enforcement of boundary conditions (**D**) and imposition of external loads (**SFE**).

3.1.2 Nodes

Nodal counters, used exclusively for node creation, are denoted as n_i and n_j . Nodes are created to accommodate n_v rows by n_u columns of 8-noded quadrilateral shell elements. $2n_v + 1$ nodal rows and $2n_u$ nodal columns are required to accommodate all elements. In reality, ' $2n_u + 1$ ' nodal columns are omitted because the ' $2n_u + 1$ ' nodal column coincides (at $u = 2\pi$) with the first one (at $u = 0$).

A nodal row is created in a loop with n_i goes from 0 to $2n_u - 1$. This loop is nested inside another loop with n_j goes from 0 to $2n_v$ to create nodal rows along the v -parameter. The loop counters are chosen to fit the required number of nodal rows and columns and to ease the calculation of the u and v parameters. The nodes are equally spaces intervals of $\frac{l_v}{2n_v}$ along v and $\frac{\pi}{n_u}$ along u . For each node, u and v are obtained from n_i and n_j using

$$u = n_i \frac{2\pi}{2n_u} \quad (31)$$

and

$$v = n_j \frac{l_v}{2n_v} \quad (32)$$

Eq.30 then yields \bar{x} , \bar{y} and \bar{z} , and the node is created via **N**. The variables t_x and t_y are introduced that, when added together, act like a Boolean indicating when a node should or should not be created. If and only if $t_x + t_y$ is less than 1, a node is created. Thus, nodes are omitted if n_i and n_j are simultaneously even. Fig.13 illustrates and elaborates the code that in charge of the node creation.

3.1.3 Elements

Element rows and columns are denoted as j and i respectively. An element column is created using a loop with i going from 1 to n_u . This loop is nested within another loop with j going from 1 to n_v element rows along the u -parameter. An element is created using **E** whose arguments are the numbers identifying the surrounding 8 nodes. Equations 33, 34 and 35 identify the numbers of the left three nodes of an element, from bottom to top, based on i and j :

$$k_1 = 1 + 2(i - 1) + 3n_u(j - 1) \quad (33)$$

$$k_2 = i + 2n_u + 3n_u(j - 1) \quad (34)$$

```

! Create shell nodes
!
! ty and tx are dummy variables that, added together, act like a Boolean
! indicating when a node should be created. If ty+tx is less than 1,
! then a node is created
ty=1
*D0,nj,0,2*nv           ! Nodal rows going from nj=0 to 2*nv
ty=-ty
tx=1
v=nj*lv/nv/2
*D0,ni,0,2*nu-1         ! Nodal columns going from ni=0 to 2*nu-1
tx=-tx
*IF,tx+ty,LT,1,THEN      ! If tx+ty=2 omit node creation
u=ni*lu/nu/2              ! Parameter u (U-V plane)
x=aa*COS(u)               ! x-coordinate x=x(u, v)
y=aa*SIN(u)               ! y-coordinate y=y(u, v)
z=v                        ! z-coordinate z=v
N,,x,y,z,,,                ! Create node
*ENDIF
*ENDDO
*ENDDO

```

Figure 13: Code of node creation

and

$$k_3 = 1 + 2(i - 1) + 3n_u j \quad (35)$$

Figure 15 shows the code that in charge of element creation.

Except the last column, the right three nodes could be expressed as equations 36, 37 and 38

$$k_4 = k_1 + 2 \quad (36)$$

$$k_5 = k_2 + 1 \quad (37)$$

and

$$k_6 = k_3 + 2 \quad (38)$$

While for the last element column, k_4 , k_5 and k_6 coincide with the first nodal column. Therefore, the expression of k_4 , k_5 and k_6 are listed below.

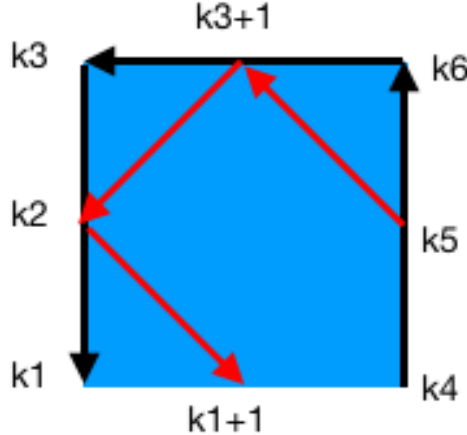


Figure 14: Element creation

$$k_4 = 1 + 3n_u(j - 1) \quad (39)$$

$$k_5 = 1 + 2n_u + 3n_u(j - 1) \quad (40)$$

and

$$k_6 = 1 + 3n_u \cdot j \quad (41)$$

3.1.4 Boundary Conditions

Fixities (Dirichlet boundary conditions) are enforced with **D**. The pressure load (Neumann boundary condition) is applied on the element using **SFE**. The bottom ring nodes are restrained against displacement in all directions, i.e., fully pinned. Therefore, the element number from 1 to $2n_u - 1$ are selected.

The uniform pressure is applied to the top ring elements and the elements close to the bottom ring to avoid the edge disturbance at the bottom. As shown in Fig.16, for the top ring elements, the external pressure is applied at the surface 4, and for the bottom ring elements, the external pressure is applied at the surface 6. The code that in charge of the creation of boundary conditions is shown in Fig.17.

The Fig.18 is a model with radius equals to 100mm, and the thickness equals to 2mm. The Young's modulus of this cylinder is 21000MPa and the Poisson's ratio equals to 0.3. This cylinder is referred as example cylinder in later.

```

! Create shell elements
! -----
SHPP, ON
*D0, j, 1, nv           ! j-th element row (along v-axis)
*D0, i, 1, nu           ! i-th element column (along u-axis)
k1=1+2*(i-1)+(j-1)*(3*nu)
k2=i+2*nu+(j-1)*3*nu
k3=1+2*(i-1)+j*(3*nu)
*IF, i, LT, nu, THEN    ! i < nu
k4=k1+2
k5=k2+1
k6=k3+2
*ELSE                   ! i = nu
k4=1+(j-1)*(3*nu)
k5=1+2*nu+(j-1)*3*nu
k6=1+j*(3*nu)
*ENDIF
E, k4, k6, k3, k1, k5, k3+1, k2, k1+1
*ENDDO
*ENDDO

```

Figure 15: Element creation code

3.2 Mechanical Analysis

ANSYS Mechanical APDL's solution procedure is preceded by **/SOLU**. The LE analysis is specified with **ANTYPE, STATIC**[1, 17]. Additionally, **PSTRES, ON** (prestress effects) is required after **ANTYPE** to save the state for the LBA[1, 17]. The code that in charge of the linear elastic analysis is shown in Fig.19.

3.2.1 Linear Buckling Analysis (LBA)

The LBA is solved using the Block Lanczos methods. ANSYS Inc. recommends requesting a few additional modes than needed to enhance the accuracy of the final solution[2, 17].

After the LBA, shell buckling results could be generated. The first buckling mode is plotted. Fig.21 shows the first linear buckling mode of the example cylinder.

Initial imperfections for the GNIA are based on Eq.21. The code uses a similar nomenclature: $\bar{\delta}$ (delta) is the prescribed imperfection amplitude and δ_{max}^k (uz_max) is the maximum deflection. The latter is obtained by looping through all the nodes and storing the largest $|u_z|$ (Fig.22). The deflections are transformed to local coordinates using *Transformation Matrix* (Fig.23).

3.2.2 Geometrically Nonlinear Analysis with Initial Geometric Imperfections (GNIA)

Geometrically nonlinear finite element analysis updates the geometry using a buckling mode and δ_{max}^k (uz_max) from section 3.2.1. The geometry is updated with **UPGEOM**, whose arguments

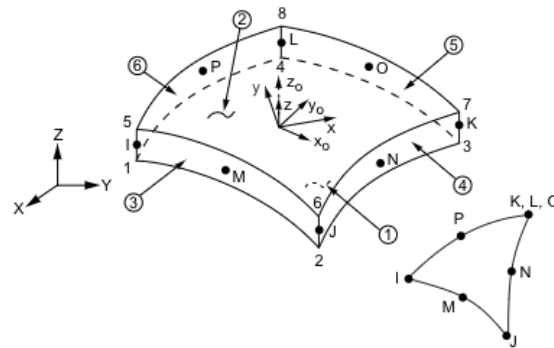


Figure 16: Shell281 Geometry[2]

```

! Create Dirichlet boundary conditions
! -----
*DO, j, 1, 2*nu
n_bot=j                                ! bottom ring
D, n_bot, UX, 0, , , UY, UZ
*ENDDO

! Create Newmann boundary conditions
! -----
! Top and bottom rings
*DO, j, 1, nu
i_top=nv*nu-j+1
ESEL, S, ELEM, , i_top, nu*nv
*ENDDO
SFE, ALL, 4, PRES, 0, p, ,
ALLSEL

*DO, j, nu+1, 2*nu
i_bot=j
ESEL, S, ELEM, , nu+1, i_bot
*ENDDO
SFE, ALL, 6, PRES, 0, p, ,
ALLSEL

```

Figure 17: Code of boundary conditions

are the factor ($\delta/\text{uz_max}$), load step, buckling mode, file and file extension is shown in Fig.24.

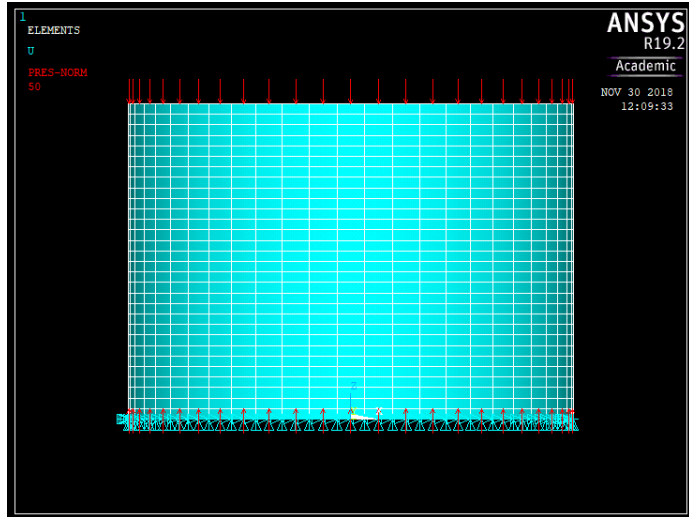


Figure 18: Model

```
! Linear Elastic Analysis
!-----
/SOLU
ANTYPE, STATIC           ! Linear elastic analysis
PSTRES, ON      ! Prestress effects to be included in buckling analysis
SOLVE
FINISH
```

Figure 19: Linear elastic analysis (LE) code

```
! Linear Buckling Analysis (Find buckling modes)
!-----
/SOLU
ANTYPE, BUCKLE          ! Linear buckling analysis
BUCOPT, LANB, 5, 0, , CENTER ! Block Lanczos method, 5 buckling modes
SOLVE
FINISH
```

Figure 20: Linear buckling analysis (LBA) code

The solution is then set up and executed as shown in Fig.25.

ANSYS Mechanical APDL uses **TIME** as the counter for both dynamic and nonlinear static anal-

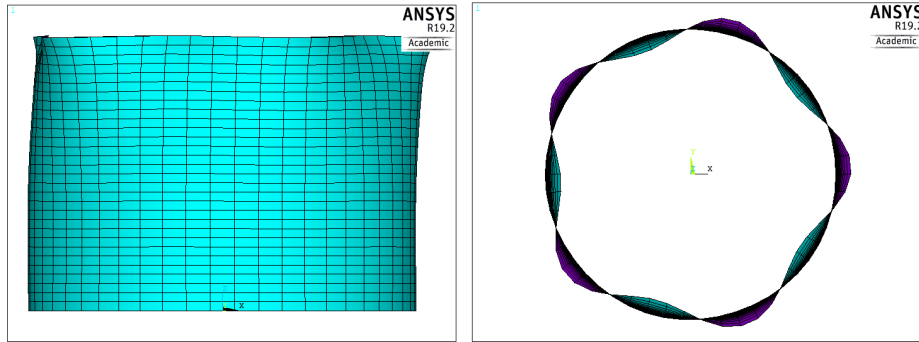


Figure 21: First linear buckling modes of the example cylinder

```

! Loop to read deflection of node next to i-th element
uz_max=0
defl_max=0
*DO, j, 1, nv           ! j-th element row (along v)
*DO, i, 1, nu+1          ! i-th element column (along u)
nnode=1+2*(i-1)+(j-1)*(3*nu+2) ! nnodes=k1(i,j)
*GET, u_x, NODE, nnodes, U, X      ! Extract u_x from nnodes
*GET, u_y, NODE, nnodes, U, Y      ! Extract u_y from nnodes
*GET, u_z, NODE, nnodes, U, Z      ! Extract u_z from nnodes
defl=SQRT(u_x*u_x+u_y*u_y+u_z*u_z) ! Absolute deflection
u=(i-1)*(lu/nu)-lu/2            ! u-parameter
v=(j-1)*(lv/nv)                 ! v-parameter
*VEC, Defl_global, D, ALLOC, 3,, , ! Assemble Gamma matrix
*SET, Defl_global(1), u_x, u_y, u_z ! Allocate space for Defl_global
*MULT, Gamma, , Defl_global, , Defl_local ! Defl_local = Gamma*Defl_global
u_z=Defl_local(3)                ! local z-displacement
*IF, ABS(u_z), GT, uz_max, THEN
  uz_max=ABS(u_z)                ! uz_max=max(u_z)
  defl_max=ABS(defl)              ! defl_max=max(defl)
  nnodes=1+2*(i-1)+(j-1)*(3*nu+2) ! node with highest deflection
*ENDIF
*ENDDO
*ENDDO

```

Figure 22: Get maximum deflection code

ysis. In a non-proportional analysis, time acts as a counter for indexing each load step. For single load step analysis, time equals λ . Assuming λ_S does not exceed 1.

```

*DMAT, Gamma, D, ALLOC, 3, 3

*VEC, i_vector, D, ALLOC, 3
i_vector(1)=-aa*SIN(u)
i_vector(2)=aa*COS(u)
i_vector(3)=0
*NRM, i_vector, NRM2, norm_i, YES

*VEC, j_vector, D, ALLOC, 3
j_vector(1)=0
j_vector(2)=0
j_vector(3)=1
*NRM, j_vector, NRM2, norm_j, YES

*VEC, m_vector, D, ALLOC, 3
m_vector(1)=i_vector(2)*j_vector(3)-i_vector(3)*j_vector(2)
m_vector(2)=i_vector(1)*j_vector(3)-i_vector(3)*j_vector(1)
m_vector(3)=i_vector(1)*j_vector(2)-i_vector(2)*j_vector(1)
*NRM, m_vector, NRM2, norm_m, YES

*D0, k, 1, 3
Gamma(1, k)=i_vector(k)
Gamma(2, k)=j_vector(k)
Gamma(3, k)=m_vector(k)
*ENDDO

```

Figure 23: Transformation Matrix

Since time defaults to 1 at the end of each analysis, the loop ensures that this value does not get saved.

```

! Update the geometry
!-----
/PREP7
FACTOR=delta/uz_max           ! Factor for UPGEOM
UPGEOM, FACTOR, 1, buckling_mode, 'file', 'rst', ! Add imperfections
/RESET $ /ERASE $ /REPLOT ! Replot
FINISH

```

Figure 24: Update the geometry code

```

/SOLU
! Set analysis type: GNA
!-----
NCNV, 0           ! Do not terminate the program if not-converged
NERR,,,-1         ! Do not terminate the program if not-converged
ANTYPE, STATIC    ! Static analysis
NLGEOM, ON         ! Nonlinear geometry

! Set nonlinear controls / solution technique
!-----
ARCLEN, ON        ! Arclength ON
nsubstep=200       ! # of substeps.
TIME, 1            ! Time at the end of load step
NSUBST, nsubstep,, ! Number of substeps
NEQIT, 1000,       ! Max. number of iterations
!CNVTOL, STAT      ! Convergence tolerance (default)

! Set output controls
!-----
RESCONTROL, DEFINE, ALL, 1      ! Write new files at every substep
OUTRES, NSOL, ALL,,,             ! Write nodal results at every substep
OUTRES, ESOL, ALL,,,             ! Write element results at every substep

! Solve
!-----
SOLVE
FINISH

```

Figure 25: Geometrically nonlinear analysis code

4 RESULTS

4.1 GNIA Results

The contour plot of the example cylinder of displacements and the third principal stresses are shown in Fig.26 and Fig.27 respectively. The load-displacement diagram (GNIA) of the example cylinder is shown in Fig.28.

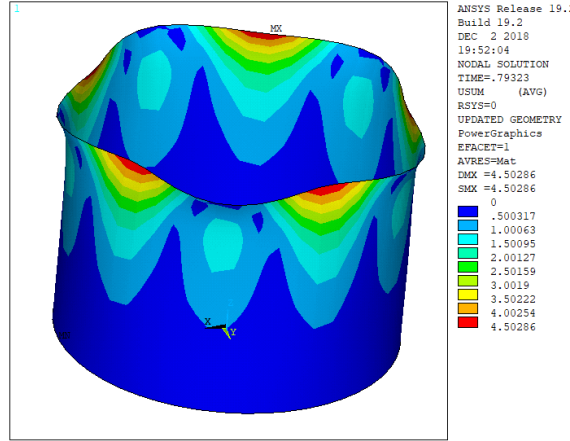


Figure 26: Contour plot of the displacements of the example cylinder

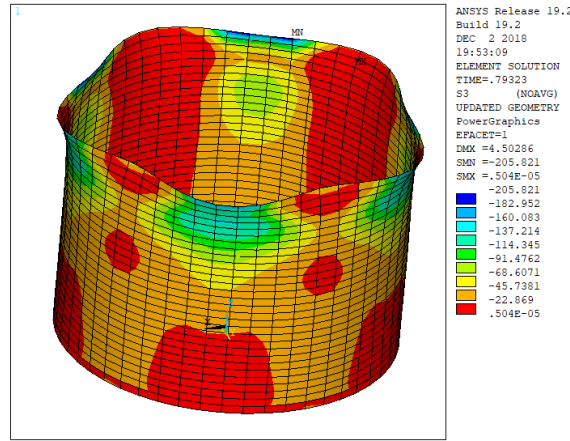


Figure 27: Contour plot of the third principal stresses of the example cylinder

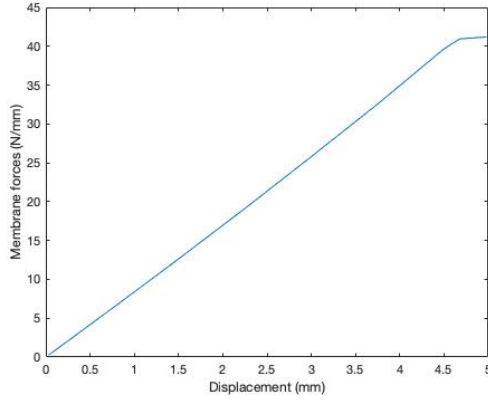


Figure 28: Membrane forces-displacement diagram of the example cylinder under GNIA

4.2 Curvatures

In order to check the relationship between the nonlinear buckling membrane forces and the curvatures of cylinders, a cylinder with thickness equals to 0.5mm , Young's modulus equals to 21000MPa and the Poisson's ratio equals to 0.3 is applied with radius varies from 15mm to 500mm . The radius of the cylinder is generated randomly. In total there are 509 cylinders are analyzed. Then the nonlinear buckling membrane forces generated with ANSYS Mechanical APDL and the nonlinear buckling membrane forces derived from Eq.1 are imported into MatLab and scatter diagrams are generated to illustrate the relation between the nonlinear buckling membrane forces and curvatures of cylinders. The numerical results are listed in App.B.

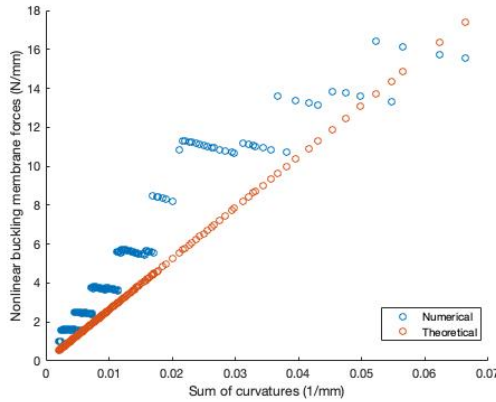


Figure 29: Nonlinear buckling membrane forces-sum of curvatures scatter diagram

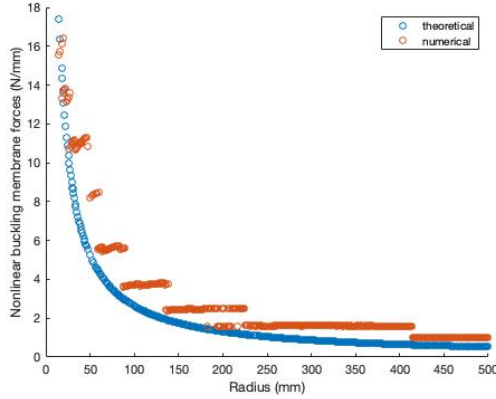


Figure 30: Nonlinear buckling membrane forces-radius scatter diagram

4.3 Thickness

In order to check the relation between nonlinear buckling membrane forces and the thickness of cylinders, a cylinder with radius equals to 100mm , Young's modulus equals to 21000MPa is applied, the thickness varies from 0.1mm to 2mm . The nonlinear buckling membrane forces generated with ANSYS Mechanical APDL and the critical membrane forces derived from Eq.1 are imported into MatLab and a scatter diagram is generated (Fig.31). The numerical results are listed in App.B

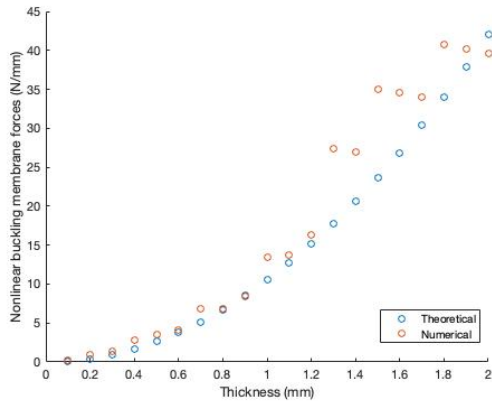


Figure 31: Nonlinear buckling membrane forces-thickness scatter diagram

4.4 Young's Modulus

In order to check the relation between nonlinear buckling membrane forces and the Young's modulus, a cylinder with thickness equals to 1mm and the radius equals to 100mm is applied, the Poisson's ratio equals to 0.3 and the Young's modulus varies from 1000MPa to 21000MPa . A scatter diagram is generated to illustrate the relationship between Young's modulus and nonlinear buckling membrane forces (Fig.32). The numerical results are listed in App.D.

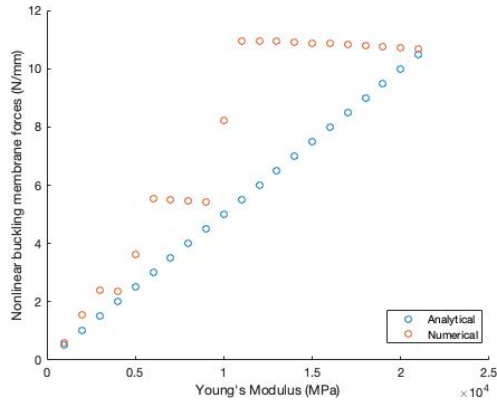


Figure 32: Nonlinear buckling membrane forces-Young's modulus diagram

4.5 Buckling Procedures

In order to improve the design of shell structures, a better understanding of shell buckling behavior is required. Therefore, a series of figures are generated for certain load steps to illustrate the shell behavior before shell buckling. The representative figures are listed below.

4.5.1 Displacements

The representative figures of the deformed shape of the example cylinder are listed below.

Fig.33 illustrates the undeformed shape of the example cylinder with initial geometric imperfections. The Gaussian curvature at the top part of the cylinder is not zero any more due to the initial geometric imperfection.

Fig.34 illustrates the how the cylinder deform. The deformation first occurs at the locations with negative Gaussian curvatures and the maximum deformation occurs at the top edge of the cylinder.

Fig.35 illustrates the deformed shape of the cylinder when buckling happens.

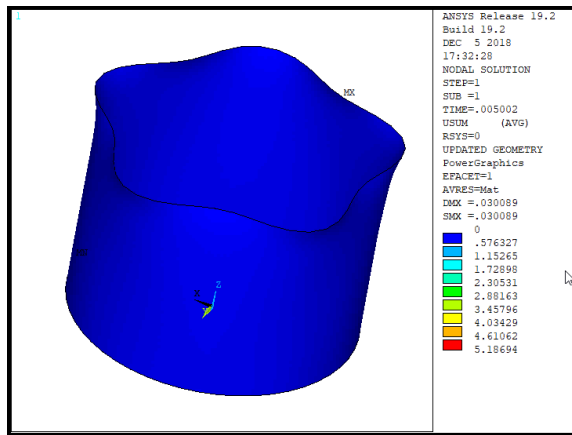


Figure 33: Undeformed cylinder with initial geometric imperfections

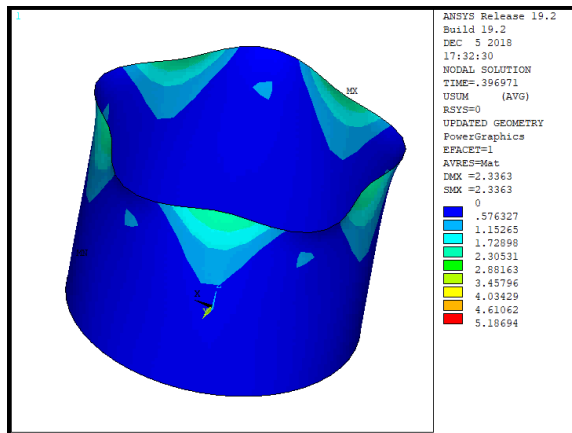


Figure 34: Deformation development of the example cylinder

4.5.2 The Third Principal Stresses

The development procedures of the third principal stresses of the example cylinder are shown in Fig.36, Fig.37, Fig.4.5.2, Fig.39 and Fig.40

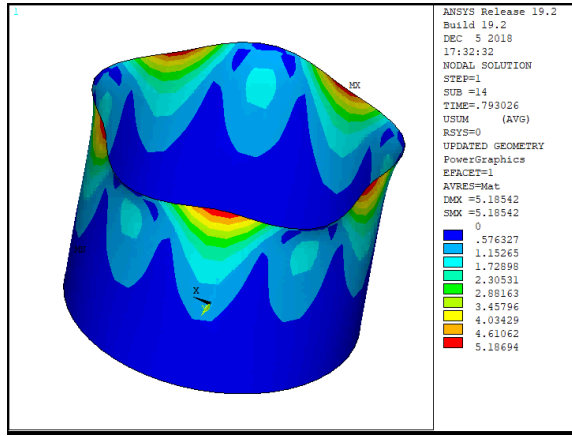


Figure 35: Deformation of the example cylinder when buckling occurs

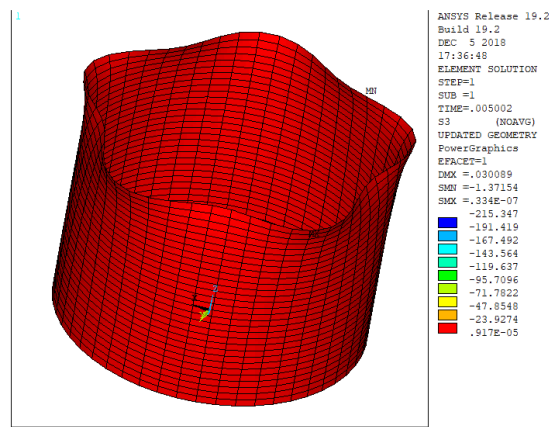


Figure 36: The third principal stresses of the example cylinder (Phase 1)

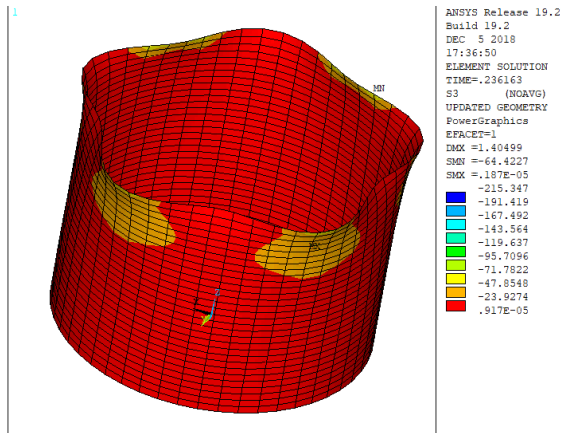


Figure 37: The third principal stresses of the example cylinder (Phase 2)

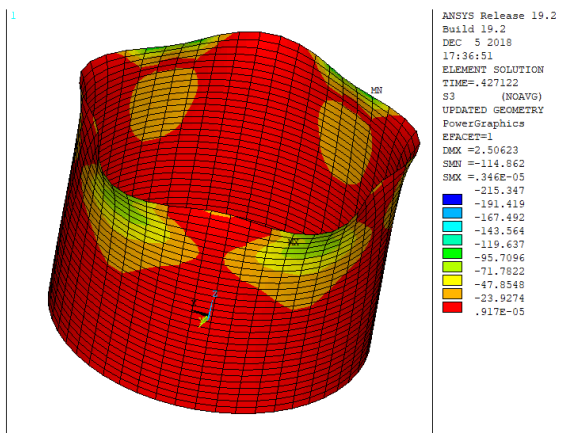


Figure 38: The third principal stresses of the example cylinder (Phase 3)

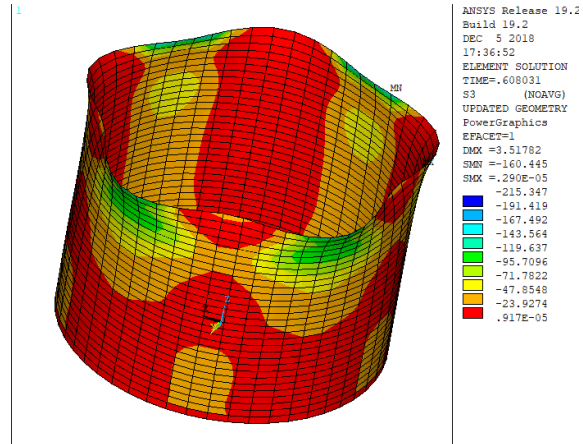


Figure 39: The third principal stresses of the example cylinder (Phase 4)

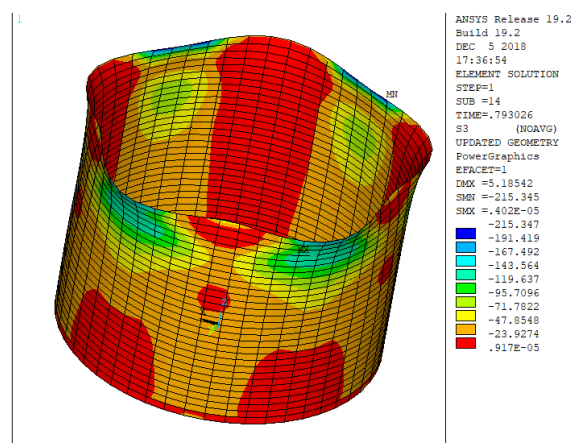


Figure 40: The third principal stresses of the example of cylinder (Phase 5)

5 DISCUSSION AND CONCLUSION

5.1 Discussion of the Correctness of the Results

Due to the existence of the initial geometric imperfections, the Gaussian curvatures of the cylinder in reality are not zero at every location. According to the Fig.33 and the Fig.34, Fig.35, it could be observed that the maximum deformation of the cylinder occurs at the location where the Gaussian curvature in reality is negative. It is reasonable as the shells with negative Gaussian curvatures have smaller capacity compared to the shells with positive Gaussian curvature when it comes to compressive membrane forces. Therefore, the deformation plots could be reliable.

According to the Fig.36, Fig.37, Fig.4.5.2, Fig.39 and Fig.40, the third principal stresses (also known as the compressive stresses) at the locations that with positive Gaussian curvatures have higher absolute value. The results are reliable as the location where the Gaussian curvature is positive is stiffer and therefore, attracts larger stresses.

According to the Fig.28, the relationship between the membrane forces and the displacements is almost linear. The diagram is reasonable as there is only geometric nonlinearity included in the finite element analysis.

Therefore, the command batches could be applied for the nonlinear buckling analysis of cylinders with ANSYS Mechanical APDL. And the database generated with ANSYS Mechanical APDL could be reliable.

5.2 Discussion of the Scatter Diagrams

5.2.1 Curvatures

According to the Fig.29 and Fig.30, a linear relationship between the sum of membrane forces and the sum of curvatures could be observed. Therefore, the relation between the nonlinear buckling membrane forces and curvatures is verified. There are some horizontal parts of the Fig.29, this is due to the variation of the curvatures is very small and the existence of the errors.

5.2.2 Thickness

As shown in Fig.31, the relation between the nonlinear buckling membrane forces of cylinders and the thickness of the cylinders is quadratic. Therefore, the formula Eq.1 is correct in terms of thickness.

5.2.3 Young's Modulus

As shown in Fig.32, the nonlinear buckling membrane forces of the cylinder is linear to the Young's modulus of the material of the cylinder. Therefore, the formula is correct in terms of the Young's modulus. The reason of the horizontal parts in the diagram is due to the material with smaller Young's modulus is more ductile, therefore, the cylinders with those materials would have a more stable performance as shell buckling in reality is a form of instability.

5.2.4 Conclusion

There are only 4 numerical results are lower than the theoretical results derived from the formula out of 550 results in total, which is 0.7273%. Thus, the formula is safe and correct.

5.3 Recommendations for Further Research

In this report, as only the cylinder is analyzed, therefore, in reality, only the relation between the n_{xx} and k_{xx} is verified, and the n_{yy} and k_{yy} have no influence in this report. Therefore, further research on the formula should focus on the combination of n_{xx} and n_{yy} , k_{xx} and k_{yy} .

Reference

- [1] ANSYS Inc. *Command Reference for the Mechanical APDL, ANSYS Manual*, 2009.
- [2] ANSYS Inc. *Theory Reference for the Mechanical APDL and Mechanical Applications*, 2009.
- [3] J. Blaauwendaard and J.H. Hoefakker. *Structural Shell Analysis: Understanding and Application (Solid Mechanics and Its Application, v.200)*. Dordrecht, the Netherlands: Springer, 2013.
- [4] R. Borst and M. Crisfield. *Nonlinear Finite Element Analysis of Solids and Structures*. Wiley series in computational mechanics. Chichester, West Sussex, United Kingdom: Wiley, 2nd ed. edition, 2012.
- [5] Bernad Budiansky and J.C. Amazigo. Initial postbuckling behavior of cylindrical shells under external pressure. *Journal of Mathematics and Physics*, 47:223–235, 1969.
- [6] Bernad Budiansky and John.W. Hutchinson. A survey of some buckling problems. *AAIA Journal*, 1505-1510, 1966.
- [7] Bushnell. Buckling of shells-pitfall for designers. *AAIA Journal*, 19(9):1183–1226, 1981.
- [8] T. Chen. On introduction imperfection in the non-linear analysis of buckling of thin-shell structures. Master’s thesis, Delft University of Technology, 2014.
- [9] D.A. Danielson. Buckling and initial postbuckling behavior of spheroidal shells under pressure. *AAIA Journal*, 7(5):936–944, 1970.
- [10] P.C.J. Hoogenboom. Cie4143 shell analysis, theory and application [lecture notes], 2018.
- [11] John.W. Hutchinson. Initial postbuckling behavior of toroidal shell segments. *International Journal of Solids and Structures*, 3:97–115, 1967.
- [12] John.W. Hutchinson. Buckling and initial postbuckling behavior of oval cylindrical shells under axial compression. *Journal of Applied Mechanics*, 35(1):66–72, 1968.
- [13] John.W. Hutchinson and W.T. Koiter. Postbuckling theory. *Applied Mechanics Reviews*, 23(12):1353–1363, 1970.
- [14] T. Kármán and H.S. Tsien. The buckling of spherical shells by external pressure. *Journal of the Aeronautical Science*, 7(2):43–50, 1939.
- [15] T. Kármán and H.S. Tsien. The buckling of thin cylindrical shells under axial compression. *Journal of the Aeronautical Science*, 8(8):303–312, 1941.
- [16] W.T. Koiter. A translation of the stability of elastic equilibrium. Technical report, STANFORD UNIV CA DEPT OF AERONAUTICS AND ASTRONAUTICS, 1970.
- [17] Erik Johannes Giesen Loo. Quantifying the influence of membrane forces, curvatures, and imperfections on the nonlinear buckling load of thin-shells. Master’s thesis, Delft University of Technology, 2017.

- [18] W. McGuire, R.H. Gallagher, and R.D. Ziemian. *Matrix Structural Analysis*. 2nd ed. edition, 2000.
- [19] G.Z. Voyatzis and P. Woelke. *Elasto-Plastic and Damage Analysis of Plates and Shells*. Berlin: Springer, 2008.
- [20] V.I. Weingarten, E.J. Morgan, and P. Seide. Elastic stability of thin-walled cylindrical and conical shells under combined internal pressure and axial compression. *AAIA Journal*, 3:500–505, 1965.
- [21] R.D. Ziemian. *Guide to Stability Design Criteria for Metal Structures*. Structural Research Council, Hoboken, N.J., U.S.: John Wiley and Sons, 2010.

A Command Lines of ANSYS Mechanical APDL (modified from [17])

```

! Preprocessing
!
/UIS, MSGPOP, 4          ! Sets pop-ups to YES
/UIS, ABORT, OFF         ! No pop-ups about status of operation in progress

t=thickness
E=Young's modulus
w=Poisson's ratio
lu=2*pi
nu=number of elements along u-axis
nv=number of elements along v-axis
p=external pressure
delta=predefined scale of initial geometric imperfections
aa=radius
lv=10*SQRT(aa*t)

/PREP7
/VIEW,ALL,0,0,0           ! All windows: camera at point (0,0,0)

! Create element type: shell
!
MP,EX,1,E                  ! Elastic modulus (linear elastic material)
MP,PRXY,1,w                 ! Poisson's ratio (linear elastic material)

! Create shell nodes
!
! ty and tx are dummy variables that, added together, act like a Boolean indicating when a node
! should be created. If ty+tx is less than 1, then a node is created.
ty=1
*DO,nj,0,2*nv               ! Nodal rows going from nj=0 to 2*nv
ty=-ty
tx-1
v=nj*lv/nv/2
*DO, ni, 0, 2*nu-1          ! Nodal columns going from ni=0 to 2*nu-1
tx=-tx
*IF,tx+ty,LT,1,THEN          ! If tx+ty=2 omit node creation
u=ni*lu/nu/2
x=aa*COS(u)                ! Parameter u (U-V Plane)
y=aa*SIN(u)                 ! x-coordinate x=x(u,v)
z=v                          ! y-coordinate y=y(u,v)
N,,x,y,z,,,                  ! z-coordinate z=z(v)
                             ! Create node

```

```

*ENDIF
*ENDDO
*ENDDO

! Create shell elements
!

SHPP,ON
*DO,j,1,nv          ! j-th element row (along v-axis)
*DO,i,1,nu          ! i-th element column (along u-axis)
k1=1+2*(i-1)+3*nu*(j-1)
k2=i+2*nu+3*nu*(j-1)
k3=1+2*(i-1)+j*3*nu
*IF,i,LT,nu,THEN      ! i<nu
k4=k1+2
k5=k2+1
k6=k3+2
*ELSE                ! i=nu
k4=1+3*nu*(j-1)
k5=1+2*nu+3*nu*(j-1)
k6=1+3*nu*k
*ENDIF
E,k4,k6,k3,k1,k5,k3+1,k2,k1+1
*ENDDO
*ENDDO

! Create Dirichlet boundary conditions
!

*DO,j,1,2*nu
n_bot=j              ! bottom ring
D,n_bot,UX,0,,,UY,UZ
*ENDDO

! Create Neumann boundary conditions
!

! Top and bottom rings
*DO,j,1,nu
i_top=nv*nu-j+1
ESEL,S,ELEM,,i_top,nu*nv
*ENDDO
SFE,ALL,4,PRES,0,p,,
ALLSEL

*DO,j,nu+1,2*nu
i_bot=j

```

```

ESEL,S,ELEM,,nu+1,i_bot
*ENDDO
SFE,ALL,6,PRES,0,p,,
ALLSEL

FINISH

! Linear Elastic Analysis
!-----
```

```

/SOLU
ANTYPE,STATIC           ! Linear elastic analysis
PSTRES,ON               ! Prestress effects to be included in buckling analysis
SOLVE
FINISH
```

```

! Transformation Matrix
!-----
```

```

*DMAT,Gamma,D,ALLOC,3,3

*VEC,i_vector,D,ALLOC,3
i_vector(1)=-aa*SIN(u)
i_vector(2)=aa*COS(u)
i_vector(3)=0
*NRM,i_vector,NRM2,norm_i,YES

*VEC,j_vector,D,ALLOC,3
j_vector(1)=0
j_vector(2)=0
j_vector(3)=1
*NRM,j_vector,NRM2,norm_j,YES

*VEC,m_vector,D,ALLOC,3
m_vector(1)=i_vector(2)*j_vector(3)-i_vector(3)*j_vector(2)
m_vector(2)=i_vector(1)*k_vector(3)-i_vector(3)*j_vector(1)
m_vector(3)=i_vector(1)*j_vector(2)-i_vector(2)*j_vector(1)
*NRM,m_vector,NRM2,norm_m,YES

*DO,k,1,3
Gamma(1,k)=i_vector(k)
Gamma(2,k)=j_vector(k)
Gamma(3,k)=m_vector(k)
*ENDDO

! Linear Buckling Analysis (Find buckling mode)
```

!

```

/SOLU
ANTYPE,BUCKLE                               ! Linear buckling analysis
BUCOPT,LANB,5,0,,CENTER                      ! Block Lanczos method, 5 buckling modes
SOLVE
FINISH

/POST1
buckling_mode=1
/RGB,INDEX,100,100,100,0
/RGB,INDEX,80,80,80,13
/RGB,INDEX,60,60,60,14
/RGB,INDEX,0,0,0,15

/WINDOW,1,LEFT
/WINDOW,2,RIGHT

/PLOPT,INFO,0
/VIEW,ALL,0,0,0
/ANGLE,ALL,0
/DIST,ALL,AUTO

/WINDOW,2,OFF
SUBSET,1,buckling_mode,FACT,,,,
/PLNSOL,U,SUM,0,1

/NOERASE
/WINDOW,1,OFF
/WINDOW,2,ON
SUBSET,1,buckling_mode+1,FACT,,,,
PLBSOL,U,SUM,0,1

SUBSET,1,buckling_mode,FACT,,,
*GET,lambdaC,ACTIVE,0,SET,FREQ
*COPEN,ShellBuckling,csv,,APPEND
*VWRITE,lambdaC
(F11.5,':,$)
*CFCLOS

! Loop to read deflection of node next to i-th element
uz_max=0
defl_max=0
*DO,j,1,nv                                ! j-th element row (along v)
*DO,i,1,nu+1                                ! i-th element column (along u)
nnode=1+2*(i-1)+(j-1)*(3*nu+2)             ! nnodes=k1(i,j)
*GET,u_x,NODE,nnode,U,X                     ! Extract u_x from nnodes

```

```

*GET,u_y,NODE,nnode,U,Y           ! Extract u_y from nnode
*GET,u_z,NODE,nnode,U,Z           ! Extract u_z from nnode
defl=SQRT(u_x*u_x+u_y*u_y+u_z*u_z) ! Absolute deflection
u=(i-1)*(lu/nu)-lu/2              ! u-parameter
v=(j-1)*(lv/nv)                  ! v-parameter
*VEC,Defl_global,D,ALLOC,3,,,
*SET,Defl_global(1),u_x,u_y,u_z   ! Assemble Gamma matrix
*MULT,Gamma,,Defl_global,,Defl_local ! Allocate space for Defl_global
u_z=Defl_local(3)                 ! Defl_local=Gamma*Defl_global
*IF,ABS(u_z),GT,uz_max,THEN      ! local z_displacement
uz_max=ABS(u_z)
defl_max=ABS(defl)
nnode=1+2*(i-1)+(j-1)*(3*nu+2)
*ENDIF
*ENDDO
*ENDDO

defl_diff=(defl_max-uz_max)/uz_max*100
*COPEN,ShellLBA,csv,,             ! uz_max=max(u_z)
*VWRITE,E,t,w,p,aa,lv,nu,nv      ! defl_max=max(defl)
(F16.4,'',F16.4,'',F16.4,'',F16.4,'',F16.4,'',F16.4,'',F16.4,'',)
*CFCLOS

*DO,j,1,nv
*DO,i,1,nu+1
nnode=1+2*(i-1)+(j-1)*(3*nu+2)
*GET,u_x,NODE,nnode,U,X
*GET,u_y,NODE,nnode,U,Y
*GET,u_z,NODE,nnode,U,Z
u=(i-1)*(lu/nu)-lu/2
v=(j-1)*(lv/nv)
*VEC,Defl_global,D,ALLOC,3,,,
*SET,Defl_global(1),u_x,u_y,u_z
*MULT,Gamma,,Defl_global,,Defl_local
u_x=Defl_local(1)
u_y=Defl_local(2)
u_z=Defl_local(3)
defl=SQRT(u_x*u_x+u_y*u_y+u_z*u_z)
*COPEN,ShellLBA,csv,,APPEND
*VWRITE,u_x,u_y,u_z,defl
(F16.8,'',F16.8,'',F16.8,'',F16.8,'',)
*CFCLOS
*ENDDO
*ENDDO

FINISH

```

```

! Update the geometry
!

/PREP7
FACTOR=delta/uz_max
UPGEOM,FACTOR,1,buckling_mode,'file','rst'           ! Factor for UPGEOM
/RESET $ /ERASE $ /REPLOT                            ! Add imperfections
FINISH                                               ! Replot

/SOLU
! Set analysis type: GNA
!

NCNV,0                                              ! Do not terminate the program if not-converged
NERR,,,,-1                                         ! Do not terminate the program if not-converged
ANTYPE,STATIC                                       ! Static analysis
NLGEOM,ON                                           ! Nonlinear geometry

! Set nonlinear controls / solution technique
!

RESCONTROL,DEFINE,ALL,1                           ! Write new files at every substep
OUTRES,NSOL,ALL,,,                                ! Write nodal results at every substep
OUTRES,ESOL,ALL,,,                                ! Write element results at every substep

! Solve
!

SOLVE
FINISH

```

B Curvatures

Table 2: Nonlinear buckling membrane forces-sum of curvatures

nxx+nyy	kxx	E	t	time	a	analytical	theoretical
20	0.00200012	21000	0.5	0.04999	499.970499	0.9998	0.52503098
20	0.00200167	21000	0.5	0.049968	499.583593	0.99936	0.52543759
20	0.00200782	21000	0.5	0.05016	498.053435	1.0032	0.52705188
20	0.002012	21000	0.5	0.049997	497.016978	0.99994	0.52815097
20	0.00201307	21000	0.5	0.050015	496.752779	1.0003	0.52843187
20	0.00201939	21000	0.5	0.049983	495.199373	0.99966	0.53008952
20	0.00202409	21000	0.5	0.049926	494.04967	0.99852	0.5313231
20	0.00202665	21000	0.5	0.049926	493.424142	0.99852	0.53199667
20	0.0020323	21000	0.5	0.049941	492.05308	0.99882	0.53347903
20	0.00203608	21000	0.5	0.049889	491.138663	0.99778	0.53447228
20	0.00203716	21000	0.5	0.049963	490.880604	0.99926	0.53475325
20	0.00204349	21000	0.5	0.050075	489.357724	1.0015	0.5364174
20	0.00205145	21000	0.5	0.050022	487.459915	1.00044	0.53850582
20	0.00205632	21000	0.5	0.050095	486.305051	1.0019	0.53978465
20	0.00205973	21000	0.5	0.050087	485.500771	1.00174	0.54067885
20	0.00206405	21000	0.5	0.050046	484.483756	1.00092	0.54181383
20	0.00207039	21000	0.5	0.05018	483.00105	1.0036	0.54347708
20	0.00207141	21000	0.5	0.05021	482.763298	1.0042	0.54374473
20	0.00207882	21000	0.5	0.050126	481.042525	1.00252	0.5456898
20	0.00208253	21000	0.5	0.050127	480.185401	1.00254	0.54666385
20	0.00208691	21000	0.5	0.050131	479.178376	1.00262	0.5478127
20	0.00209192	21000	0.5	0.050167	478.029265	1.00334	0.54912956
20	0.00209594	21000	0.5	0.05022	477.112982	1.0044	0.55018415
20	0.00210049	21000	0.5	0.05018	476.078387	1.0036	0.55137979
20	0.0021046	21000	0.5	0.050218	475.14916	1.00436	0.5524581
20	0.00210752	21000	0.5	0.050209	474.491813	1.00418	0.55322346
20	0.00211143	21000	0.5	0.050213	473.612006	1.00426	0.55425115
20	0.00211816	21000	0.5	0.050231	472.106924	1.00462	0.55601811
20	0.00212254	21000	0.5	0.050259	471.133788	1.00518	0.55716658
20	0.00212571	21000	0.5	0.050256	470.430271	1.00512	0.55799981
20	0.00212764	21000	0.5	0.050286	470.005258	1.00572	0.55850439
20	0.00212864	21000	0.5	0.050315	469.784033	1.0063	0.55876739
20	0.00213372	21000	0.5	0.050324	468.664617	1.00648	0.56010202
20	0.00214081	21000	0.5	0.050222	467.11367	1.00444	0.56196172
20	0.0021447	21000	0.5	0.050244	466.265602	1.00488	0.56298384
20	0.00215038	21000	0.5	0.050256	465.03453	1.00512	0.56447421
20	0.00215338	21000	0.5	0.050256	464.386025	1.00512	0.56526249

continued on next page

nxx+nyy	kxx	E	t	time	a	analytical	theoretical
20	0.00215733	21000	0.5	0.050256	463.536979	1.00512	0.56629786
20	0.00216416	21000	0.5	0.050237	462.073615	1.00474	0.5680913
20	0.00216725	21000	0.5	0.050238	461.414986	1.00476	0.5689022
20	0.00217373	21000	0.5	0.05042	460.038919	1.0084	0.5706039
20	0.0021783	21000	0.5	0.050376	459.073251	1.00752	0.57180417
20	0.00218227	21000	0.5	0.050478	458.238024	1.00956	0.57284639
20	0.00218454	21000	0.5	0.050286	457.762107	1.00572	0.57344196
20	0.00219256	21000	0.5	0.050368	456.088057	1.00736	0.57554675
20	0.00219723	21000	0.5	0.050474	455.117607	1.00948	0.57677399
20	0.00219862	21000	0.5	0.05047	454.831529	1.0094	0.57713677
20	0.00220609	21000	0.5	0.050574	453.290879	1.01148	0.57909835
20	0.00221028	21000	0.5	0.050528	452.431187	1.01056	0.58019873
20	0.00221232	21000	0.5	0.05049	452.013518	1.0098	0.58073484
20	0.00221781	21000	0.5	0.050496	450.895931	1.00992	0.58217425
20	0.00222062	21000	0.5	0.050471	450.324698	1.00942	0.58291273
20	0.00222582	21000	0.5	0.050577	449.27322	1.01154	0.58427698
20	0.00223069	21000	0.5	0.050536	448.292224	1.01072	0.58555555
20	0.00223309	21000	0.5	0.050502	447.809199	1.01004	0.58618715
20	0.00223927	21000	0.5	0.050508	446.574427	1.01016	0.58780795
20	0.00224585	21000	0.5	0.050469	445.265742	1.00938	0.58953559
20	0.00224851	21000	0.5	0.050459	444.739546	1.00918	0.5902331
20	0.00225731	21000	0.5	0.050387	443.004253	1.00774	0.5925451
20	0.00226222	21000	0.5	0.050456	442.044548	1.00912	0.59383155
20	0.00226597	21000	0.5	0.050525	441.311972	1.0105	0.59481731
20	0.00227039	21000	0.5	0.050579	440.45386	1.01158	0.59597616
20	0.00227532	21000	0.5	0.05045	439.499091	1.009	0.59727086
20	0.002282	21000	0.5	0.050535	438.211504	1.0107	0.59902581
20	0.002287	21000	0.5	0.050623	437.254177	1.01246	0.60033732
20	0.00229391	21000	0.5	0.050542	435.93756	1.01084	0.60215045
20	0.00229433	21000	0.5	0.050491	435.857608	1.00982	0.60226091
20	0.00230344	21000	0.5	5.06E-02	434.133161	1.01160954	0.60465319
20	0.00230822	21000	0.5	0.050551	433.234733	1.01102	0.6059071
20	0.00231223	21000	0.5	0.050647	432.483119	1.01294	0.60696011
20	0.00231603	21000	0.5	0.050537	431.773306	1.01074	0.60795792
20	0.00232523	21000	0.5	0.050947	430.065049	1.01894	0.61037278
20	0.0023302	21000	0.5	0.050649	429.147516	1.01298	0.61167778
20	0.00233469	21000	0.5	0.050674	428.321563	1.01348	0.61285731
20	0.00234241	21000	0.5	0.05054	426.91052	1.0108	0.61488295
20	0.00234276	21000	0.5	0.050542	426.84646	1.01084	0.61497523
20	0.00235187	21000	0.5	0.050552	425.193642	1.01104	0.61736577

continued on next page

nxx+nyy	kxx	E	t	time	a	analytical	theoretical
20	0.0023567	21000	0.5	0.050607	424.321948	1.01214	0.61863404
20	0.00235924	21000	0.5	0.05056	423.866129	1.0112	0.61929931
20	0.00236931	21000	0.5	0.050643	422.063597	1.01286	0.62194419
20	0.00237397	21000	0.5	0.050718	421.23591	1.01436	0.62316624
20	0.00237923	21000	0.5	0.050767	420.304744	1.01534	0.62454684
20	0.00238641	21000	0.5	0.050729	419.039537	1.01458	0.62643254
20	0.00239186	21000	0.5	0.050661	418.084633	1.01322	0.62786331
20	0.00239684	21000	0.5	0.050602	417.216811	1.01204	0.62916928
20	0.00240197	21000	0.5	0.050603	416.324796	1.01206	0.63051733
20	0.00240932	21000	0.5	0.050609	415.054149	1.01218	0.6324476
20	0.00241372	21000	0.5	0.050841	414.297782	1.01682	0.63360223
20	0.00241972	21000	0.5	0.078963	413.270279	1.57926	0.63517754
20	0.00242545	21000	0.5	0.078986	412.2948	1.57972	0.63668036
20	0.00243257	21000	0.5	0.079149	411.087248	1.58298	0.63855058
20	0.00243588	21000	0.5	0.078992	410.528929	1.57984	0.63941901
20	0.00244333	21000	0.5	0.079026	409.277851	1.58052	0.64137358
20	0.00244953	21000	0.5	0.079078	408.241365	1.58156	0.64300197
20	0.00245776	21000	0.5	0.079093	406.875186	1.58186	0.64516099
20	0.00245835	21000	0.5	0.079194	406.776181	1.58388	0.64531802
20	0.00246634	21000	0.5	0.079143	405.459355	1.58286	0.64741384
20	0.00247452	21000	0.5	0.079242	404.118656	1.58484	0.6495617
20	0.00248132	21000	0.5	0.079172	403.010747	1.58344	0.6513474
20	0.0024838	21000	0.5	0.079181	402.608677	1.58362	0.65199787
20	0.0024937	21000	0.5	0.07922	401.010433	1.5844	0.65459644
20	0.00249775	21000	0.5	0.079345	400.360094	1.5869	0.65565975
20	0.00250264	21000	0.5	0.07927	399.578782	1.5854	0.65694179
20	0.00250872	21000	0.5	0.079278	398.609263	1.58556	0.65853964
20	0.00251854	21000	0.5	0.0793	397.055632	1.586	0.66111642
20	0.00252357	21000	0.5	0.07939	396.263349	1.5878	0.66243825
20	0.0025293	21000	0.5	0.079457	395.365757	1.58914	0.66394217
20	0.00253801	21000	0.5	0.079588	394.008917	1.59176	0.66622858
20	0.00254431	21000	0.5	0.07939	393.03372	1.5878	0.66788163
20	0.00254864	21000	0.5	0.079462	392.366495	1.58924	0.66901737
20	0.0025558	21000	0.5	0.0797	391.266301	1.594	0.67089857
20	0.00255808	21000	0.5	0.079699	390.917877	1.59398	0.67149654
20	0.00256827	21000	0.5	0.080025	389.367905	1.6005	0.67416959
20	0.00257355	21000	0.5	0.079799	388.568206	1.59598	0.67555707
20	0.00258155	21000	0.5	0.080194	387.364418	1.60388	0.67765646
20	0.00258905	21000	0.5	0.079662	386.242547	1.59324	0.67962476
20	0.00259782	21000	0.5	7.97E-02	384.938077	1.59392	0.68192786

continued on next page

nxx+nyy	kxx	E	t	time	a	analytical	theoretical
20	0.00260376	21000	0.5	7.97E-02	384.060038	1.5947	0.68348689
20	0.00260876	21000	0.5	0.079751	383.323199	1.59502	0.68480071
20	0.00261779	21000	0.5	0.079794	382.0013	1.59588	0.68717044
20	0.00262436	21000	0.5	0.079819	381.045122	1.59638	0.68889479
20	0.00262802	21000	0.5	0.07985	380.514385	1.597	0.68985565
20	0.0026325	21000	0.5	0.079859	379.867705	1.59718	0.69103005
20	0.00264166	21000	0.5	0.079867	378.549754	1.59734	0.69343593
20	0.00264807	21000	0.5	0.07989	377.632912	1.5978	0.6951195
20	0.00265637	21000	0.5	0.080056	376.45295	1.60112	0.69729829
20	0.00266394	21000	0.5	0.080068	375.384121	1.60136	0.69928371
20	0.00266689	21000	0.5	0.079943	374.967957	1.59886	0.70005982
20	0.00267333	21000	0.5	0.080076	374.065409	1.60152	0.70174893
20	0.0026805	21000	0.5	0.080161	373.064057	1.60322	0.70363251
20	0.00268632	21000	0.5	0.080267	372.256055	1.60534	0.70515979
20	0.00269381	21000	0.5	0.080147	371.220931	1.60294	0.70712607
20	0.00269719	21000	0.5	0.080324	370.755871	1.60648	0.70801306
20	0.00270279	21000	0.5	0.080391	369.987511	1.60782	0.70948341
20	0.0027156	21000	0.5	0.080708	368.242688	1.61416	0.71284511
20	0.00272363	21000	0.5	0.080461	367.156607	1.60922	0.71495377
20	0.00272844	21000	0.5	0.08077	366.509148	1.6154	0.71621678
20	0.00273655	21000	0.5	0.080301	365.423496	1.60602	0.71834461
20	0.00274403	21000	0.5	0.080654	364.427903	1.61308	0.72030708
20	0.002753	21000	0.5	0.080192	363.24009	1.60384	0.72266252
20	0.00276101	21000	0.5	0.08021	362.186759	1.6042	0.72476421
20	0.00276516	21000	0.5	0.080287	361.642642	1.60574	0.72585467
20	0.0027767	21000	0.5	0.08053	360.139481	1.6106	0.72888426
20	0.00278346	21000	0.5	0.08029	359.264867	1.6058	0.7306587
20	0.00279186	21000	0.5	0.080285	358.18468	1.6057	0.73286217
20	0.00279666	21000	0.5	0.080498	357.568778	1.60996	0.7341245
20	0.00280531	21000	0.5	0.08028	356.46695	1.6056	0.73639365
20	0.0028119	21000	0.5	0.080703	355.631821	1.61406	0.73812293
20	0.00282281	21000	0.5	0.080469	354.256302	1.60938	0.74098893
20	0.00283043	21000	0.5	0.080678	353.303361	1.61356	0.74298755
20	0.00283739	21000	0.5	0.080617	352.437117	1.61234	0.74481372
20	0.00284586	21000	0.5	0.080807	351.387703	1.61614	0.74703809
20	0.00285598	21000	0.5	0.080426	350.143104	1.60852	0.74969347
20	0.00286371	21000	0.5	0.080373	349.196809	1.60746	0.75172508
20	0.00286681	21000	0.5	0.080368	348.819547	1.60736	0.7525381
20	0.002878	21000	0.5	0.080386	347.463411	1.60772	0.75547523
20	0.00288889	21000	0.5	0.080448	346.154015	1.60896	0.75833296

continued on next page

nxx+nyy	kxx	E	t	time	a	analytical	theoretical
20	0.00289584	21000	0.5	0.080474	345.3234	1.60948	0.760157
20	0.00290122	21000	0.5	0.080532	344.682832	1.61064	0.7615697
20	0.00290998	21000	0.5	0.080532	343.64529	1.61064	0.76386905
20	0.00291819	21000	0.5	0.080505	342.678379	1.6101	0.7660244
20	0.00293134	21000	0.5	0.08051	341.140926	1.6102	0.76947672
20	0.00293674	21000	0.5	0.080574	340.514059	1.61148	0.77089328
20	0.00294827	21000	0.5	0.080594	339.182415	1.61188	0.77391984
20	0.00295577	21000	0.5	0.080627	338.321404	1.61254	0.77588943
20	0.00296099	21000	0.5	0.0808	337.724686	1.616	0.77726033
20	0.00296961	21000	0.5	0.080401	336.744157	1.60802	0.77952355
20	0.00298243	21000	0.5	0.080431	335.29734	1.60862	0.78288721
20	0.00299122	21000	0.5	0.080747	334.312108	1.61494	0.78519441
20	0.00299818	21000	0.5	0.080581	333.535499	1.61162	0.78702267
20	0.00301052	21000	0.5	0.080599	332.167989	1.61198	0.79026278
20	0.00301343	21000	0.5	0.080629	331.847757	1.61258	0.79102538
20	0.00302854	21000	0.5	0.080629	330.191924	1.61258	0.79499219
20	0.00303666	21000	0.5	0.080484	329.309409	1.60968	0.79712268
20	0.00304405	21000	0.5	0.080487	328.509791	1.60974	0.79906294
20	0.0030559	21000	0.5	0.080662	327.235909	1.61324	0.80217358
20	0.00306718	21000	0.5	0.080746	326.032816	1.61492	0.80513368
20	0.0030691	21000	0.5	0.08093	325.828269	1.6186	0.80563912
20	0.00308174	21000	0.5	0.080551	324.491926	1.61102	0.80895695
20	0.00309511	21000	0.5	0.08069	323.090103	1.6138	0.81246686
20	0.00309996	21000	0.5	0.080559	322.585108	1.61118	0.81373874
20	0.0031112	21000	0.5	0.080734	321.419163	1.61468	0.81669057
20	0.00312215	21000	0.5	0.080598	320.291935	1.61196	0.81956481
20	0.00313064	21000	0.5	0.0806854	319.423607	1.613708	0.82179274
20	0.00313364	21000	0.5	0.080591	319.117818	1.61182	0.8225802
20	0.00314229	21000	0.5	0.080617	318.238806	1.61234	0.82485226
20	0.00314882	21000	0.5	0.080724	317.579702	1.61448	0.82656416
20	0.00315887	21000	0.5	0.080644	316.569273	1.61288	0.8292024
20	0.00317037	21000	0.5	0.080633	315.42057	1.61266	0.8322222
20	0.00317154	21000	0.5	0.08094	315.304307	1.6188	0.83252906
20	0.00318032	21000	0.5	0.080784	314.434	1.61568	0.83483338
20	0.00318995	21000	0.5	0.08083	313.484266	1.6166	0.8373626
20	0.00320049	21000	0.5	0.08088	312.451702	1.6176	0.84012985
20	0.00321249	21000	0.5	0.080677	311.284838	1.61354	0.84327911
20	0.0032232	21000	0.5	0.080623	310.2505	1.61246	0.8460905
20	0.00323263	21000	0.5	0.080768	309.345224	1.61536	0.84856652
20	0.00324063	21000	0.5	0.080886	308.581768	1.61772	0.85066594

continued on next page

nxx+nyy	kxx	E	t	time	a	analytical	theoretical
20	0.00325526	21000	0.5	0.080651	307.195539	1.61302	0.8545046
20	0.00326452	21000	0.5	0.080626	306.323756	1.61252	0.85693648
20	0.00327527	21000	0.5	0.080992	305.318463	1.61984	0.85975803
20	0.00328775	21000	0.5	0.080987	304.159454	1.61974	0.86303416
20	0.00329456	21000	0.5	0.080905	303.531055	1.6181	0.8648209
20	0.003309	21000	0.5	0.080641	302.206534	1.61282	0.86861127
20	0.00331544	21000	0.5	0.080946	301.619536	1.61892	0.87030172
20	0.00331887	21000	0.5	0.08061	301.307422	1.6122	0.87120323
20	0.00332247	21000	0.5	0.080719	300.980583	1.61438	0.87214928
20	0.00334041	21000	0.5	0.080594	299.364226	1.61188	0.87685828
20	0.00334936	21000	0.5	0.080537	298.564556	1.61074	0.87920684
20	0.00336086	21000	0.5	0.08088	297.543166	1.6176	0.88222493
20	0.00337072	21000	0.5	0.080587	296.67222	1.61174	0.8848149
20	0.00338828	21000	0.5	0.080605	295.134717	1.6121	0.88942434
20	0.00339555	21000	0.5	0.080986	294.503409	1.61972	0.89133094
20	0.00340944	21000	0.5	0.080653	293.302928	1.61306	0.89497913
20	0.0034189	21000	0.5	0.080559	292.491659	1.61118	0.89746149
20	0.00342903	21000	0.5	0.08056	291.627797	1.6112	0.90011996
20	0.00344252	21000	0.5	0.080557	290.485129	1.61114	0.90366072
20	0.00345261	21000	0.5	0.080496	289.635668	1.60992	0.90631103
20	0.00346432	21000	0.5	0.08045	288.657107	1.609	0.90938346
20	0.0034806	21000	0.5	0.081512	287.306483	1.63024	0.91365847
20	0.00349638	21000	0.5	0.08147	286.009718	1.6294	0.91780098
20	0.00350234	21000	0.5	0.081476	285.523717	1.62952	0.91936321
20	0.0035125	21000	0.5	0.081462	284.697849	1.62924	0.92203015
20	0.00352797	21000	0.5	0.081448	283.449112	1.62896	0.92609216
20	0.00353735	21000	0.5	0.081467	282.697439	1.62934	0.92855457
20	0.00354031	21000	0.5	0.081408	282.461451	1.62816	0.92933035
20	0.00355434	21000	0.5	0.081407	281.34633	1.62814	0.93301377
20	0.00356459	21000	0.5	0.081393	280.537205	1.62786	0.93570477
20	0.00357667	21000	0.5	0.081375	279.589785	1.6275	0.9388755
20	0.00358882	21000	0.5	0.08118	278.642874	1.6236	0.94206608
20	0.00359132	21000	0.5	0.08139	278.449119	1.6278	0.9427216
20	0.00360383	21000	0.5	0.081375	277.482447	1.6275	0.94600578
20	0.00361002	21000	0.5	0.081365	277.006746	1.6273	0.94763035
20	0.00361937	21000	0.5	0.081373	276.291199	1.62746	0.95008455
20	0.00362956	21000	0.5	0.081392	275.515547	1.62784	0.9527593
20	0.00364002	21000	0.5	0.081323	274.723656	1.62646	0.95550563
20	0.00365397	21000	0.5	0.081302	273.675184	1.62604	0.95916625
20	0.00367363	21000	0.5	0.081228	272.210049	1.62456	0.96432884

continued on next page

nxx+nyy	kxx	E	t	time	a	analytical	theoretical
20	0.00369942	21000	0.5	0.08107	270.312902	1.6214	0.97109682
20	0.00370759	21000	0.5	0.080784	269.716956	1.61568	0.97324248
20	0.00371315	21000	0.5	0.080927	269.313045	1.61854	0.97470213
20	0.00371625	21000	0.5	0.080795	269.088445	1.6159	0.97551569
20	0.00372208	21000	0.5	0.080722	268.666646	1.61444	0.97704722
20	0.00373983	21000	0.5	0.080747	267.391851	1.61494	0.98170531
20	0.00375282	21000	0.5	0.080671	266.466156	1.61342	0.98511572
20	0.00376758	21000	0.5	0.080648	265.422079	1.61296	0.98899082
20	0.00377869	21000	0.5	0.080681	264.64188	1.61362	0.9919065
20	0.00380051	21000	0.5	0.080604	263.122824	1.61208	0.99763295
20	0.00380977	21000	0.5	0.080563	262.482701	1.61126	1.00006591
20	0.00382801	21000	0.5	0.080583	261.232484	1.61166	1.00485206
20	0.00384239	21000	0.5	0.08054	260.254613	1.6108	1.00862765
20	0.00385436	21000	0.5	0.080451	259.446461	1.60902	1.01176944
20	0.00386676	21000	0.5	0.080536	258.614642	1.61072	1.01502373
20	0.00388191	21000	0.5	0.08045	257.604902	1.609	1.01900235
20	0.00389382	21000	0.5	0.080457	256.817494	1.60914	1.02212663
20	0.0039159	21000	0.5	0.080401	255.368814	1.60802	1.02792505
20	0.00392498	21000	0.5	0.080432	254.778423	1.60864	1.03030703
20	0.00393076	21000	0.5	0.080389	254.403929	1.60778	1.03182369
20	0.00393719	21000	0.5	0.080372	253.987932	1.60744	1.03351367
20	0.00394592	21000	0.5	0.080476	253.426193	1.60952	1.03580453
20	0.00395857	21000	0.5	0.080349	252.616476	1.60698	1.03912462
20	0.0039828	21000	0.5	0.080315	251.079599	1.6063	1.04548518
20	0.00399236	21000	0.5	0.080236	250.478704	1.60472	1.04799329
20	0.00400996	21000	0.5	0.080251	249.378868	1.60502	1.05261525
20	0.00402791	21000	0.5	0.080317	248.267598	1.60634	1.05732686
20	0.0040445	21000	0.5	0.080142	247.249254	1.60284	1.06168167
20	0.00405735	21000	0.5	0.080108	246.466387	1.60216	1.06505395
20	0.00407653	21000	0.5	0.080191	245.306386	1.60382	1.07009037
20	0.00408851	21000	0.5	0.080245	244.587714	1.6049	1.07323461
20	0.00410619	21000	0.5	0.080016	243.53483	1.60032	1.07787457
20	0.00412145	21000	0.5	0.080869	242.633156	1.61738	1.08188017
20	0.00413471	21000	0.5	0.080695	241.854853	1.6139	1.08536172
20	0.00416334	21000	0.5	0.080666	240.191696	1.61332	1.09287708
20	0.004196	21000	0.5	0.080728	238.321944	1.61456	1.10145124
20	0.0042096	21000	0.5	0.080442	237.552151	1.60884	1.10502052
20	0.00422459	21000	0.5	0.080409	236.709621	1.60818	1.10895366
20	0.0042509	21000	0.5	0.080769	235.244154	1.61538	1.11586195
20	0.00426458	21000	0.5	0.08106	234.489687	1.6212	1.11945222

continued on next page

nxx+nyy	kxx	E	t	time	a	analytical	theoretical
20	0.00428042	21000	0.5	0.080549	233.622089	1.61098	1.12360951
20	0.00430482	21000	0.5	0.080395	232.297959	1.6079	1.13001423
20	0.00432468	21000	0.5	0.080397	231.231208	1.60794	1.13522739
20	0.00435077	21000	0.5	0.08063	229.84418	1.6126	1.14207808
20	0.0043783	21000	0.5	0.080703	228.399102	1.61406	1.14930399
20	0.00439085	21000	0.5	0.0806	227.746572	1.612	1.15259693
20	0.00441593	21000	0.5	0.08055	226.45262	1.611	1.15918288
20	0.00442802	21000	0.5	0.080539	225.834704	1.61078	1.16235457
20	0.00443303	21000	0.5	0.080556	225.579202	1.61112	1.16367111
20	0.00445188	21000	0.5	0.125068	224.624407	2.50136	1.16861744
20	0.00449497	21000	0.5	0.125123	222.470735	2.50246	1.17993047
20	0.00450745	21000	0.5	0.125216	221.855081	2.50432	1.18320482
20	0.00452999	21000	0.5	0.125047	220.751003	2.50094	1.18912257
20	0.00455186	21000	0.5	0.124886	219.690431	2.49772	1.19486315
20	0.00457078	21000	0.5	0.124836	218.781197	2.49672	1.19982889
20	0.00460337	21000	0.5	0.12488	217.232081	2.4976	1.20838506
20	0.00462498	21000	0.5	0.079757	216.217299	1.59514	1.21405642
20	0.00464791	21000	0.5	0.124784	215.15039	2.49568	1.2200768
20	0.0046702	21000	0.5	0.124735	214.123674	2.4947	1.22592703
20	0.00468975	21000	0.5	0.124762	213.231164	2.49524	1.23105833
20	0.00471302	21000	0.5	0.124743	212.177984	2.49486	1.23716889
20	0.00472854	21000	0.5	0.124766	211.481597	2.49532	1.24124275
20	0.00474956	21000	0.5	0.12462	210.545945	2.4924	1.24675876
20	0.00477434	21000	0.5	0.079339	209.453246	1.58678	1.25326298
20	0.00480058	21000	0.5	0.079276	208.308313	1.58552	1.26015134
20	0.00481686	21000	0.5	0.124445	207.604209	2.4889	1.26442523
20	0.00482962	21000	0.5	0.079182	207.055645	1.58364	1.26777514
20	0.00484824	21000	0.5	0.079112	206.260441	1.58224	1.27266284
20	0.00484895	21000	0.5	0.124159	206.230342	2.48318	1.27284859
20	0.00487012	21000	0.5	0.079051	205.33389	1.58102	1.27840562
20	0.00488331	21000	0.5	0.078905	204.779275	1.5781	1.281868
20	0.00492581	21000	0.5	0.078862	203.012279	1.57724	1.29302523
20	0.00494798	21000	0.5	0.078788	202.102571	1.57576	1.29884542
20	0.0049583	21000	0.5	0.12599	201.682134	2.5198	1.30155307
20	0.00496706	21000	0.5	0.080211	201.326258	1.60422	1.30385377
20	0.00499242	21000	0.5	0.125987	200.303641	2.51974	1.31051038
20	0.00502186	21000	0.5	0.125282	199.129261	2.50564	1.31823921
20	0.00503601	21000	0.5	0.125513	198.569802	2.51026	1.32195327
20	0.00506688	21000	0.5	0.08016	197.359996	1.6032	1.33005678
20	0.00509115	21000	0.5	0.079975	196.419395	1.5995	1.33642607

continued on next page

nxx+nyy	kxx	E	t	time	a	analytical	theoretical
20	0.00510044	21000	0.5	0.080074	196.061586	1.60148	1.33886503
20	0.00512696	21000	0.5	0.079913	195.047436	1.59826	1.34582646
20	0.00514537	21000	0.5	0.079908	194.349296	1.59816	1.35066092
20	0.00517225	21000	0.5	0.1254	193.339421	2.508	1.35771587
20	0.00517794	21000	0.5	0.125476	193.126872	2.50952	1.35921012
20	0.00520445	21000	0.5	0.124495	192.143242	2.4899	1.36616827
20	0.00521719	21000	0.5	0.124948	191.6739	2.49896	1.36951353
20	0.00523893	21000	0.5	0.12483	190.878648	2.4966	1.37521929
20	0.00526974	21000	0.5	0.124699	189.762594	2.49398	1.3833074
20	0.0053188	21000	0.5	0.124513	188.012161	2.49026	1.39618628
20	0.00534079	21000	0.5	0.124452	187.23828	2.48904	1.40195691
20	0.00537175	21000	0.5	0.124364	186.159219	2.48728	1.41008327
20	0.00538266	21000	0.5	0.124326	185.781915	2.48652	1.412947
20	0.00541275	21000	0.5	0.124236	184.749138	2.48472	1.4208456
20	0.00546292	21000	0.5	0.124105	183.052364	2.4821	1.43401589
20	0.00548093	21000	0.5	0.078736	182.450946	1.57472	1.43874288
20	0.00549615	21000	0.5	0.123988	181.945528	2.47976	1.4427395
20	0.00555067	21000	0.5	0.123828	180.158404	2.47656	1.4570511
20	0.00557982	21000	0.5	0.123733	179.217163	2.47466	1.46470347
20	0.00562319	21000	0.5	0.123586	177.835011	2.47172	1.47608729
20	0.00564251	21000	0.5	0.123541	177.226163	2.47082	1.48115829
20	0.00565905	21000	0.5	0.123474	176.70821	2.46948	1.48549974
20	0.00566749	21000	0.5	0.123501	176.444942	2.47002	1.48771621
20	0.00569977	21000	0.5	0.123563	175.445738	2.47126	1.4961891
20	0.00573934	21000	0.5	0.123256	174.236209	2.46512	1.50657548
20	0.00577202	21000	0.5	0.123127	173.249578	2.46254	1.51515521
20	0.00578841	21000	0.5	0.123124	172.759049	2.46248	1.51945731
20	0.00583382	21000	0.5	0.122872	171.414165	2.45744	1.53137869
20	0.00586166	21000	0.5	0.122797	170.600053	2.45594	1.53868651
20	0.00590999	21000	0.5	0.122584	169.20513	2.45168	1.5513714
20	0.00591543	21000	0.5	0.122553	169.049448	2.45106	1.5528001
20	0.00593054	21000	0.5	0.122515	168.618684	2.4503	1.55676698
20	0.00597679	21000	0.5	0.122333	167.313813	2.44666	1.56890812
20	0.00598373	21000	0.5	0.122295	167.119935	2.4459	1.57072824
20	0.0060094	21000	0.5	0.122177	166.405933	2.44354	1.5774678
20	0.00604685	21000	0.5	0.124745	165.375495	2.4949	1.58729683
20	0.00608447	21000	0.5	0.124679	164.35288	2.49358	1.59717311
20	0.00611789	21000	0.5	0.124387	163.455038	2.48774	1.60594622
20	0.00617135	21000	0.5	0.124618	162.039173	2.49236	1.61997864
20	0.00620071	21000	0.5	0.123994	161.271727	2.47988	1.62768766

continued on next page

nxx+nyy	kxx	E	t	time	a	analytical	theoretical
20	0.00623677	21000	0.5	0.123888	160.339414	2.47776	1.63715204
20	0.00628305	21000	0.5	0.123476	159.15838	2.46952	1.64930053
20	0.00632833	21000	0.5	0.123525	158.019485	2.4705	1.66118755
20	0.00636809	21000	0.5	0.12354	157.032968	2.4708	1.6716235
20	0.00644988	21000	0.5	0.123267	155.041606	2.46534	1.69309392
20	0.00648826	21000	0.5	0.123102	154.124514	2.46204	1.70316839
20	0.00652678	21000	0.5	0.122928	153.214896	2.45856	1.71327989
20	0.00657655	21000	0.5	0.122769	152.055479	2.45538	1.72634358
20	0.00662182	21000	0.5	0.12276	151.015907	2.4552	1.73822748
20	0.00663251	21000	0.5	0.122767	150.772443	2.45534	1.74103433
20	0.00669116	21000	0.5	0.122407	149.450865	2.44814	1.75643011
20	0.00674276	21000	0.5	0.122257	148.307247	2.44514	1.76997419
20	0.00679844	21000	0.5	0.122127	147.092519	2.44254	1.7845911
20	0.00683438	21000	0.5	0.121968	146.318946	2.43936	1.79402604
20	0.0068816	21000	0.5	0.121791	145.31512	2.43582	1.80641904
20	0.00692184	21000	0.5	0.121639	144.47036	2.43278	1.8169817
20	0.00698455	21000	0.5	0.121387	143.173047	2.42774	1.83344564
20	0.00701896	21000	0.5	0.121248	142.471279	2.42496	1.84247662
20	0.00707491	21000	0.5	0.121065	141.34448	2.4213	1.85716485
20	0.00711176	21000	0.5	0.120936	140.612136	2.41872	1.86683744
20	0.00716083	21000	0.5	0.120761	139.648703	2.41522	1.87971671
20	0.00721179	21000	0.5	0.187707	138.661851	3.75414	1.89309459
20	0.00729813	21000	0.5	0.120186	137.021336	2.40372	1.91576005
20	0.00734722	21000	0.5	0.122098	136.105972	2.44196	1.92864424
20	0.00735766	21000	0.5	0.187072	135.912845	3.74144	1.93138477
20	0.00745497	21000	0.5	0.18661	134.138615	3.7322	1.95693089
20	0.00751132	21000	0.5	0.19062	133.132387	3.8124	1.97172157
20	0.0075693	21000	0.5	0.19044866	132.112583	3.80897328	1.98694169
20	0.00762601	21000	0.5	0.19019	131.130237	3.8038	2.00182663
20	0.00768959	21000	0.5	0.190191	130.045994	3.80382	2.01851662
20	0.00775181	21000	0.5	0.189695	129.002193	3.7939	2.03484912
20	0.00780947	21000	0.5	0.189816	128.049654	3.79632	2.04998602
20	0.00785779	21000	0.5	0.189405	127.262213	3.7881	2.06267041
20	0.0079199	21000	0.5	0.189473	126.264257	3.78946	2.07897315
20	0.00798912	21000	0.5	0.189288	125.17027	3.78576	2.09714336
20	0.00806337	21000	0.5	0.188995	124.017626	3.7799	2.11663461
20	0.00811101	21000	0.5	0.188825	123.289181	3.7765	2.12914059
20	0.00819497	21000	0.5	0.18847	122.026131	3.7694	2.15117858
20	0.00824507	21000	0.5	0.187779	121.284563	3.75558	2.1643315
20	0.00831733	21000	0.5	0.188209	120.23093	3.76418	2.18329843

continued on next page

nxx+nyy	kxx	E	t	time	a	analytical	theoretical
20	0.00838763	21000	0.5	0.187675	119.223183	3.7535	2.201753
20	0.00846221	21000	0.5	0.187393	118.172498	3.74786	2.22132902
20	0.00853508	21000	0.5	0.18714	117.163572	3.7428	2.24045747
20	0.00860509	21000	0.5	0.186854	116.210264	3.73708	2.25883663
20	0.0086905	21000	0.5	0.186075	115.068183	3.7215	2.28125615
20	0.00875869	21000	0.5	0.186152	114.172375	3.72304	2.29915512
20	0.00882844	21000	0.5	0.185963	113.270345	3.71926	2.31746447
20	0.00892784	21000	0.5	0.18545	112.009165	3.709	2.34355822
20	0.00899856	21000	0.5	0.185106	111.12884	3.70212	2.3621231
20	0.00907058	21000	0.5	0.184261	110.246569	3.68522	2.38102648
20	0.00912324	21000	0.5	0.184702	109.610206	3.69404	2.39484999
20	0.00925153	21000	0.5	0.184192	108.090251	3.68384	2.42852613
20	0.00934464	21000	0.5	0.183789	107.013217	3.67578	2.45296803
20	0.009384	21000	0.5	0.183632	106.56439	3.67264	2.46329942
20	0.00949874	21000	0.5	0.188803	105.27715	3.77606	2.49341855
20	0.00960234	21000	0.5	0.187724	104.141298	3.75448	2.52061387
20	0.00961795	21000	0.5	0.18782	103.97231	3.7564	2.52471066
20	0.00968472	21000	0.5	0.187534	103.255422	3.75068	2.54223938
20	0.00978704	21000	0.5	0.187323	102.175939	3.74646	2.56909801
20	0.00984838	21000	0.5	0.18693	101.53953	3.7386	2.58520006
20	0.00999343	21000	0.5	0.186563	100.065772	3.73126	2.62327462
20	0.01007988	21000	0.5	0.186257	99.2075288	3.72514	2.64596854
20	0.01015072	21000	0.5	0.185954	98.515197	3.71908	2.66456352
20	0.01030511	21000	0.5	0.18532	97.0392381	3.7064	2.70509131
20	0.01031587	21000	0.5	0.185261	96.9379798	3.70522	2.70791696
20	0.01051999	21000	0.5	0.18446	95.0571572	3.6892	2.76149643
20	0.01060731	21000	0.5	0.184043	94.2745705	3.68086	2.78442001
20	0.01074209	21000	0.5	0.183676	93.0917886	3.67352	2.81979758
20	0.01082993	21000	0.5	0.183363	92.3366981	3.66726	2.84285669
20	0.01096489	21000	0.5	0.182875	91.2001971	3.6575	2.87828325
20	0.01109652	21000	0.5	0.182426	90.1183151	3.64852	2.91283742
20	0.01119816	21000	0.5	0.281699	89.3004221	5.63398	2.93951578
20	0.01121277	21000	0.5	0.281628	89.1840365	5.63256	2.94335186
20	0.01121294	21000	0.5	0.281616	89.1826889	5.63232	2.94339634
20	0.01130758	21000	0.5	0.281166	88.4362342	5.62332	2.96824036
20	0.01134419	21000	0.5	0.280993	88.1508748	5.61986	2.97784906
20	0.01139435	21000	0.5	0.18128	87.7627623	3.6256	2.99101798
20	0.01140727	21000	0.5	0.280699	87.6633587	5.61398	2.99440957
20	0.01140908	21000	0.5	0.180983	87.6494955	3.61966	2.99488318
20	0.01145687	21000	0.5	0.18073	87.2838804	3.6146	3.00742816

continued on next page

nxx+nyy	kxx	E	t	time	a	analytical	theoretical
20	0.01156951	21000	0.5	0.279916	86.4340803	5.59832	3.03699651
20	0.01175735	21000	0.5	0.278899	85.0531749	5.57798	3.08630454
20	0.01189636	21000	0.5	0.278037	84.0593119	5.56074	3.12279501
20	0.01200956	21000	0.5	0.285388	83.2670145	5.70776	3.15250885
20	0.01218304	21000	0.5	0.287066	82.0813182	5.74132	3.19804806
20	0.01228469	21000	0.5	0.286794	81.4021339	5.73588	3.22473119
20	0.01244581	21000	0.5	0.285769	80.3483218	5.71538	3.2670253
20	0.01265309	21000	0.5	0.284777	79.0320556	5.69554	3.32143708
20	0.01279354	21000	0.5	0.284155	78.1644486	5.6831	3.35830425
20	0.01282286	21000	0.5	0.28423	77.9857443	5.6846	3.3659998
20	0.01298164	21000	0.5	0.283474	77.0318784	5.66948	3.40768011
20	0.01306594	21000	0.5	0.283135	76.5348427	5.6627	3.42981041
20	0.01331729	21000	0.5	0.28204	75.0903425	5.6408	3.49578909
20	0.01351431	21000	0.5	0.28118	73.9956489	5.6236	3.54750589
20	0.01369556	21000	0.5	0.280253	73.0163765	5.60506	3.59508391
20	0.01387975	21000	0.5	0.279559	72.0474085	5.59118	3.64343431
20	0.01398386	21000	0.5	0.278909	71.5110009	5.57818	3.67076389
20	0.01425147	21000	0.5	0.277496	70.1681947	5.54992	3.74101117
20	0.01447467	21000	0.5	0.276896	69.0862155	5.53792	3.79960022
20	0.01461066	21000	0.5	0.27588	68.4431733	5.5176	3.8352985
20	0.01481222	21000	0.5	0.27545	67.5118299	5.509	3.88820745
20	0.01517543	21000	0.5	0.274287	65.8960063	5.48574	3.98354946
20	0.01540718	21000	0.5	0.273288	64.9047845	5.46576	4.04438598
20	0.01561208	21000	0.5	0.27252	64.0529672	5.4504	4.09817081
20	0.01575149	21000	0.5	0.28285	63.4860654	5.657	4.13476561
20	0.01604555	21000	0.5	0.281842	62.322568	5.63684	4.21195738
20	0.01616133	21000	0.5	0.281461	61.8760826	5.62922	4.24235002
20	0.0163615	21000	0.5	0.280666	61.1191072	5.61332	4.29489258
20	0.01665641	21000	0.5	0.279704	60.0369558	5.59408	4.37230697
20	0.01670272	21000	0.5	0.279486	59.870473	5.58972	4.38446511
20	0.01684356	21000	0.5	0.424664	59.3698649	8.49328	4.42143502
20	0.01698571	21000	0.5	0.278411	58.8730303	5.56822	4.4587479
20	0.01710244	21000	0.5	0.277989	58.4711835	5.55978	4.48939092
20	0.01751678	21000	0.5	0.422028	57.0881026	8.44056	4.59815597
20	0.01770538	21000	0.5	0.42122	56.4800002	8.4244	4.64766288
20	0.01843042	21000	0.5	0.4176	54.2581118	8.352	4.83798627
20	0.01904004	21000	0.5	0.414659	52.5209046	8.29318	4.99800988
20	0.02002609	21000	0.5	0.410184	49.9348501	8.20368	5.25684966
20	0.02105927	21000	0.5	0.542391	47.4850197	10.84782	5.5280592
20	0.02172547	21000	0.5	0.565788	46.0289263	11.31576	5.70293554

continued on next page

nxx+nyy	kxx	E	t	time	a	analytical	theoretical
20	0.0220105	21000	0.5	0.56424	45.4328604	11.2848	5.77775641
20	0.02264587	21000	0.5	0.562806	44.1581658	11.25612	5.94454038
20	0.0230772	21000	0.5	0.56137	43.3328048	11.2274	6.05776619
20	0.02376944	21000	0.5	0.558798	42.070824	11.17596	6.23947845
20	0.02438112	21000	0.5	0.555937	41.0153449	11.11874	6.4000437
20	0.02495012	21000	0.5	0.553447	40.0799728	11.06894	6.54940564
20	0.02551941	21000	0.5	0.551174	39.1858596	11.02348	6.69884501
20	0.02625424	21000	0.5	0.548189	38.089091	10.96378	6.89173706
20	0.02668879	21000	0.5	0.546388	37.4689194	10.92776	7.00580653
20	0.02750609	21000	0.5	0.543103	36.3555888	10.86206	7.22034793
20	0.02835911	21000	0.5	0.539926	35.2620318	10.79852	7.44426758
20	0.02938637	21000	0.5	0.536279	34.0293769	10.72558	7.71392321
20	0.0298439	21000	0.5	0.534747	33.5076823	10.69494	7.83402437
20	0.03120274	21000	0.5	0.558439	32.0484705	11.16878	8.19071849
20	0.0321394	21000	0.5	0.55535	31.1144568	11.107	8.43659273
20	0.03286608	21000	0.5	0.552885	30.4265108	11.0577	8.6273448
20	0.03320454	21000	0.5	5.52E-01	30.1163622	11.03552	8.71619215
20	0.0343449	21000	0.5	0.547743	29.1164036	10.95486	9.01553653
20	0.03568094	21000	0.5	0.543344	28.0261713	10.86688	9.36624548
20	0.03664591	21000	0.5	0.678919	27.2881747	13.57838	9.61955142
20	0.03803401	21000	0.5	0.535698	26.2922566	10.71396	9.98392811
20	0.03953274	21000	0.5	0.668868	25.2954917	13.37736	10.3773432
20	0.04157688	21000	0.5	0.663273	24.0518314	13.26546	10.9139298
20	0.04305908	21000	0.5	0.657208	23.2239051	13.14416	11.3030087
20	0.04533648	21000	0.5	0.692611	22.0572932	13.85222	11.9008256
20	0.04743336	21000	0.5	0.687611	21.082208	13.75222	12.4512575
20	0.04978492	21000	0.5	0.679748	20.0864057	13.59496	13.0685402
20	0.05231091	21000	0.5	0.819762	19.1164718	16.39524	13.7316134
20	0.05464844	21000	0.5	0.666351	18.2987839	13.32702	14.3452156
20	0.05655518	21000	0.5	0.80575	17.6818472	16.115	14.845734
20	0.06231851	21000	0.5	0.786134	16.0465966	15.72268	16.358609
20	0.06631073	21000	0.5	0.776534	15.0805152	15.53068	17.4065671

C Thickness

Table 3: Nonlinear buckling membran forces-thickness

t	a	kxx+kyy	theoretical	lambda	analytical	nxx+nyy
0.1	100	0.01	0.105	0.031251	0.156255	5
0.2	100	0.01	0.42	0.189254	0.94627	5
0.3	100	0.01	0.945	0.280145	1.400725	5
0.4	100	0.01	1.68	0.565498	2.82749	5
0.5	100	0.01	2.625	0.691437	3.457185	5
0.6	100	0.01	3.78	0.807102	4.03551	5
0.7	100	0.01	5.145	0.68383	6.8383	10
0.8	100	0.01	6.72	0.687292	6.87292	10
0.9	100	0.01	8.505	0.837072	8.37072	10
1	100	0.01	10.5	0.674114	13.48228	20
1.1	100	0.01	12.705	0.688121	13.76242	20
1.2	100	0.01	15.12	0.817772	16.35544	20
1.3	100	0.01	17.745	0.548856	27.4428	50
1.4	100	0.01	20.58	0.539131	26.95655	50
1.5	100	0.01	23.625	0.700406	35.0203	50
1.6	100	0.01	26.88	0.691273	34.56365	50
1.7	100	0.01	30.345	0.68089	34.0445	50
1.8	100	0.01	34.02	0.815976	40.7988	50
1.9	100	0.01	37.905	0.80368	40.184	50
2	100	0.01	42	0.793236	39.6618	50

D Young's Modulus

Table 4: Nonlinear buckling membrane forces-Young's modulus

E	t	a	kx+kyy	lambda	theoretical	analytical	nxx+nyy
21000	1	100	0.01	0.534597	10.5	10.69194	20
20000	1	100	0.01	0.535664	10	10.71328	20
19000	1	100	0.01	0.538002	9.5	10.76004	20
18000	1	100	0.01	0.539247	9	10.78494	20
17000	1	100	0.01	0.54116	8.5	10.8232	20
16000	1	100	0.01	0.54267	8	10.8534	20
15000	1	100	0.01	0.544407	7.5	10.88814	20
14000	1	100	0.01	0.545753	7	10.91506	20
13000	1	100	0.01	0.547246	6.5	10.94492	20
12000	1	100	0.01	0.547815	6	10.9563	20
11000	1	100	0.01	0.547676	5.5	10.95352	20
10000	1	100	0.01	0.411124	5	8.22248	20
9000	1	100	0.01	0.27104	4.5	5.4208	20
8000	1	100	0.01	0.272958	4	5.45916	20
7000	1	100	0.01	0.274915	3.5	5.4983	20
6000	1	100	0.01	0.277114	3	5.54228	20
5000	1	100	0.01	0.181058	2.5	3.62116	20
4000	1	100	0.01	0.11778	2	2.3556	20
3000	1	100	0.01	0.119985	1.5	2.3997	20
2000	1	100	0.01	0.07844	1	1.5688	20
1000	1	100	0.01	0.030313	0.5	0.60626	20